An Exemplar International APM Treaty Compliance Inspection Program

Cite as: Freitas RA Jr. An Exemplar International APM Treaty Compliance Inspection Program. IMM Report No. 61, July 2025; http://www.imm.org/Reports/rep061.pdf.

Table of Contents

1. Introduction

The advent of nanofactories[1] capable of manufacturing nanorobots and other atomically precise products will usher in an age of unprecedented opportunity and potential risk for humanity. Employed peacefully, molecular manufacturing and nanorobots can:

(1) reverse and cure all medical sequelae of injury, disease, infirmity, aging, and death;[2]

(2) revive patients from cryopreservation after legal death;[3]

(3) provide access to almost inexhaustible sources of clean energy[4] and inexpensive food production;[5]

(4) create nanocomputers that are billions of times more energy-efficient than present-day computer systems (e.g., 10^{12} GFLOPS/watt);[6]

(5) clear all man-made toxins from the environment[7] and restore the atmospheric composition to pristine pre-industrial levels,[8] ending the threat of global warming;

---

[1] Drexler KE. Nanosystems: Molecular Machinery, Manufacturing, and Computation. John Wiley & Sons, New York, 1992; https://www.amazon.com/dp/0471575186/. Freitas RA Jr., Merkle RC. A Nanofactory Roadmap: Research Proposal for a Comprehensive Diamondoid Nanofactory Development Program. IMM Report No. 58, 2008/2025; http://www.imm.org/Reports/rep058.pdf.

[2] Freitas RA Jr. Chapter 23. Comprehensive Nanorobotic Control of Human Morbidity and Aging. In: Fahy GM, West MD, Coles LS, Harris SB, eds, The Future of Aging: Pathways to Human Life Extension, Springer, New York, 2010; http://www.nanomedicine.com/Papers/Aging.pdf.

[3] Freitas RA Jr. Cryostasis Revival: The Recovery of Cryonics Patients through Nanomedicine. Alcor Life Extension Foundation, Scottsdale AZ, 2022; https://www.alcor.org/cryostasis-revival/.

[4] Freitas RA Jr., Nanomedicine, Volume I: Basic Capabilities, Landes Bioscience, Georgetown, TX, 1999, Chapter 6, "Power"; http://www.nanomedicine.com/NMI/6.1.htm. Freitas RA Jr. Energy Density. IMM Report No. 50, 25 Jun 2019; http://www.imm.org/Reports/rep050.pdf.

[5] e.g., Freitas RA Jr. The Whiskey Machine: Nanofactory-Based Replication of Fine Spirits and Other Alcohol-Based Beverages. IMM Report No. 47, May 2016; http://www.imm.org/Reports/rep047.pdf.

[6] Merkle RC, Freitas RA Jr., Hogg T, Moore TE, Moses MS, Ryley J. Mechanical computing systems using only links and rotary joints. J Mechanisms Robotics 2018 Dec;10(6):061006; https://arxiv.org/pdf/1801.03534. Merkle RC, Freitas RA Jr., Hogg T, Moore TE, Moses MS, Ryley J. Molecular mechanical computing systems. IMM Report No. 46, Apr 2016; http://www.imm.org/Reports/rep046.pdf. Merkle RC, Freitas RA Jr., Allis DG. Design of a molecular Field Effect Transistor (mFET). IMM Report No. 56, 13 Mar 2025; http://www.imm.org/Reports/rep056.pdf.

[7] Drexler KE, Peterson C, Pergamit G. Unbounding the Future. Chapter 9, "Restoring the Environment", William Morrow, NY, 1991; https://foresight.org/unbounding-the-future/utf-chapter-9-restoring-the-environment/. Freitas RA Jr. Nanofactory-Based Environmental Remediation: Cleanup of Polluted Oil Sands Tailings Pond Water in Alberta, Canada. IMM Report No. 51, 10 April 2023; http://www.imm.org/Reports/rep051.pdf.

[8] Freitas RA Jr. Diamond Trees (Tropostats): A Molecular Manufacturing Based System for Compositional Atmospheric Homeostasis. IMM Report No. 43, Feb 2010;

(6) provide a radical abundance of materials and manufactured goods (whether large or small, simple or complex) to the people of Earth at a cost of $1/kg or less;[9] and

(7) provide cheap transportation to anywhere on Earth, or even to interplanetary space.[10]

Many of these beneficial uses could have significant positive but also negative economic impacts on existing business operations.[11] Of even greater concern, sophisticated nanorobots manufactured in nanofactories could enable mass exterminations,[12] totalitarian mind control,[13] or worse[14] if employed maliciously or as instruments of politics or war.

It is therefore anticipated that when nanofactories capable of manufacturing nanorobots and other atomically precise products become available, there will arise a need to extensively regulate the manufacture and use of these devices. This regulation will have to be negotiated internationally, and will likely involve treaty obligations among all civilized countries in the world. To be effective in fact, such treaty(ies) must necessarily include inspection and enforcement provisions. These provisions will require the employment of nanorobotic devices capable of performing the inspection functions as part of a comprehensive treaty compliance monitoring effort. The present

---

http://www.imm.org/Reports/rep043.pdf. Freitas RA Jr. The Nanofactory Solution to Global Climate Change: Atmospheric Carbon Capture. IMM Report No. 45, Dec 2015; http://www.imm.org/Reports/rep045.pdf.

[9] Freitas RA Jr., Merkle RC. Kinematic Self-Replicating Machines. Landes Bioscience, Georgetown, TX, 2004; http://www.MolecularAssembler.com/KSRM.htm. Freitas RA Jr. Economic Impact of the Personal Nanofactory. Nanotechnology Perceptions: A Review of Ultraprecision Engineering and Nanotechnology 2006 May;2:111-126; http://www.rfreitas.com/Nano/NoninflationaryPN.pdf.

[10] Drexler KE. Molecular manufacturing for space systems: an overview. J Brit Interplanet Soc. 1992;45(10):401-405; https://citeseerx.ist.psu.edu/document?repid=rep1&type=pdf&doi=bbd185724f0cb7ab52c6d004573a0a45b8eb8ea6. McKendree T. Implications of Molecular Nanotechnology: Technical Performance Parameters on Previously Defined Space System Architectures. 4th Foresight Conference on Molecular Nanotechnology, Nov 1995; https://www.zyvex.com/nanotech/nano4/mckendreePaper.html. Globus A, Bailey D, Han J, Jaffe R, Levit C, Merkle R, Srivastava D. NASA applications of molecular nanotechnology. J Brit Interplanet Soc. 1998;51:145-152; https://www.nas.nasa.gov/assets/nas/pdf/techreports/1997/nas-97-029.pdf.

[11] Freitas RA Jr. Economic Impact of the Personal Nanofactory. Nanotechnology Perceptions: A Review of Ultraprecision Engineering and Nanotechnology 2006 May;2:111-126; http://www.rfreitas.com/Nano/NoninflationaryPN.pdf.

[12] Freitas RA Jr. Some Limits to Global Ecophagy by Biovorous Nanoreplicators, with Public Policy Recommendations. Zyvex Corporation, Apr 2000; http://www.rfreitas.com/Nano/Ecophagy.htm.

[13] Freitas RA Jr. What Price Freedom? Nanotechnology Perceptions: A Review of Ultraprecision Engineering and Nanotechnology 2006 May;2:99-106; http://www.rfreitas.com/Nano/WhatPriceFreedom.pdf.

[14] Drexler KE. Engines of Creation, Doubleday, 1986, Chapter 11, “Engines of Destruction,” pp. 172-177; https://web.archive.org/web/20030212122242/https://foresight.org/EOC/EOC_Chapter_11.html.

document considers a few key aspects of one possible technical implementation of a monitoring effort supporting an international treaty regime that could be put in place to establish and maintain a strict international regulatory system concerning the design, construction, and operation of **atomically precise manufacturing** (APM) facilities, also known as nanofactories.

In order to properly monitor treaty compliance as part of a comprehensive APM Treaty Compliance Inspection Program,[15] a core premise of this paper is that mobile nanorobotic inspection devices may be deployed that are capable of entering any facility, whether conventionally secure or otherwise, and detecting or inferring the presence or operation of nanotechnology equipment that is proscribed by Treaty for that particular facility operator. Such proscribed equipment might include unregulated operating nanofactories of any kind, unregulated nanofactories under construction but not yet in operation, activities that would appear to represent a technological development ramp towards an unregulated nanofactory, or equipment performing measurements, experiments, or other research or development work that could lead to the creation of either an unregulated nanofactory or equipment capable of manufacturing unregulated nanorobots or other unregulated atomically precise devices and products. Scanning probe microscope (SPM) equipment,[16] dewars of liquid nitrogen (LN2) or liquid helium (LHe),[17] and the like might also raise incremental suspicion and require further investigation.[18]

When a Treaty violation is detected by the inspection devices, the responses could range from silently reporting the infraction to the APM Treaty Compliance Inspection Program authority, at the passive end of the response spectrum, to active disablement of the offending technology by other agencies, at the more interventionist end of the response spectrum. Determination of the proper response to an observed Treaty violation, along with deciding which authority might appropriately take responsibility for making that decision, is beyond the scope of this document.

It should be noted that the capabilities described in this document, while sufficient to detect the existence or operation of proscribed nanotechnology equipment, also make possible an unprecedented invasion of privacy at the facilities and among the personnel who are subjected to

---

[15] It is unclear how a multilateral international Treaty enabling an APM Compliance Inspection Program as described herein might be negotiated. The classic concept of "national technical means" (https://en.wikipedia.org/wiki/National_technical_means_of_verification) has generally been understood to mean surveillance satellites, signal intelligence, and related capabilities with some flexibility in interpretation. The technical means proposed here are considerably more intrusive and as such may be more challenging to gain international acceptance. However, the practical legal and political genesis of the APM Treaty Compliance Inspection Program is beyond the scope of this document.

[16] https://en.wikipedia.org/wiki/Scanning_probe_microscopy.
[17] https://en.wikipedia.org/wiki/Cryogenic_storage_dewar.

[18] The present document focuses exclusively on the positional-assembly- and scanning-probe-based technical pathway to nanofactories and nanorobotics that has been pursued by this author and others over the last several decades. The success of other approaches to atomically precise manufacturing such as DNA nanotechnology, biotechnology, or self-assembly cannot be conclusively ruled out. Such possible alternative technical pathways to nanofactories and nanorobotics should be examined and explored in future analyses, and the milestones and equipment requirements for those alternative approaches should be added to the list of surveillance targets contemplated in this document.

scrutiny. Inspections should be as minimally invasive as necessary to conclusively ascertain the absence or presence of proscribed APM equipment and processes. Appropriate legal, ethical and technical safeguards must be designed and implemented in order to restrict the use of any information acquired under Treaty auspices to the appropriate Treaty personnel, solely for legally sanctioned enforcement purposes.[19]

This document[20] summarizes the overall inspection program and mission objectives (Section 2), then describes the inspection devices and the tasks they must perform (Section 3), including mapping and inspecting facilities suspected of harboring or operating unauthorized atomically precise manufacturing facilities or their precursors. A representative mission scenario is briefly outlined in Section 4.

The basic inspection mission may be supplemented by various generic methods intended to detect observable outbreaks of nanotechnology-based free-range replicators,[21] such as high-resolution thermal signature surveillance from low Earth orbit, direct soil sampling, and other means as described elsewhere.[22]

The author thanks Thomas McKendree for suggestions and comments on an earlier version of this manuscript.

---

[19] Both revelations and future suspicions of intelligence misuse may reasonably be anticipated and must be planned for in advance. This potentially calls for additional means of external verification to ensure that any intelligence produced by the APM Treaty Compliance Inspection Program is gathered and used strictly for appropriate purposes. Designing such means of external verification that may be acceptable to all Treaty signatories and good-faith stakeholders may be a difficult implementation problem and is beyond the scope of this document.

[20] Regarding the **possible future classification of this document:** It should be noted that in the National Security realm a technical description in sufficient detail to allow the design of countermeasures against a real capability can be classified. This document was entirely generated without any awareness of or access to any classified information. This document is entirely the product of open-source information and analysis.

[21] Freitas RA Jr., Merkle RC. Kinematic Self-Replicating Machines. Landes Bioscience, Georgetown, TX, 2004; http://www.MolecularAssembler.com/KSRM.htm.

[22] Drexler KE. Engines of Creation, Doubleday, 1986, “Active Shields”, pp. 187-8; https://web.archive.org/web/20030212122242/https://foresight.org/EOC/EOC_Chapter_11.html#section04of05. Freitas RA Jr. Some Limits to Global Ecophagy by Biovorous Nanoreplicators, with Public Policy Recommendations. Zyvex Corporation, Apr 2000; http://www.rfreitas.com/Nano/Ecophagy.htm. Vassar M, Freitas RA Jr. Lifeboat Foundation NanoShield Proposal. Lifeboat Foundation, Jul 2006; http://lifeboat.com/ex/nanoshield.

2. Program and Mission Objectives

The basic objective of the APM Treaty Compliance Inspection Program will be to ensure that no atomically precise manufacturing facilities, or nanofactories, either exist or are under active development, or are operated, outside of the regulatory parameters of the Treaty, anywhere in the world. If any such facilities are found, their location and the nature of their activities must be reported to the APM Treaty Compliance Inspection Program authority for appropriate action by other agencies.

Achievement of the objectives of the APM Treaty Compliance Inspection Program is made feasible by the Program's access to authorized regulated nanofactories and the nanorobotic instrumentalities that such nanofactories can manufacture. For the purposes of this document, it will be assumed that all facilities which are the subject of inspection either: (1) are authorized regulated facilities that must abide by strict protocols providing complete transparency to APM Treaty Compliance Inspection Program inspection instrumentalities; or (2) do not yet have access to nanorobotic instrumentalities as sophisticated as those possessed by the Inspection Program authorities, that could be used to block effective inspections (i.e., we assume that regulatory inspection authorities possess a persistent technological advantage).

This document describes methods of inspection primarily aimed at the detection of unregistered covert APM facilities and operations. Similar methods of inspection could be employed to undertake ongoing surveillance of specific sites of enduring concern. Regulated facilities that are registered with the APM Treaty Compliance Inspection Program will also receive periodic validation inspections to ensure that they are complying with all Treaty safety regulations, but this may require different and perhaps easier methods of assessment (e.g., cooperative physical inspections and records auditing).

Unregulated facilities may exist either within the borders of Treaty signatory countries, in which case local governmental permission to freely inspect suspect facilities may be presumed, or within countries that are not signatories to the Treaty, wherein the inspection of suspect facilities must proceed with or without official local governmental approval. Suspect facilities located in well-hidden secret locations or isolated extreme wilderness areas (including remote high-altitude mountaintops, deep oceanic floors, floating atmospheric sites, or outer space) present special situations that must also be addressed but which lie beyond the scope of the present document.

2.1 Unregulated Suspect Facilities

Unregulated suspect facilities might be found in:

* University laboratories, located on campus or in university-owned property;
* Corporate laboratories located in company buildings or research parks;
* Corporate campus complexes or company "retreat" facilities;
* Leased commercial facilities;
* Research labs owned or operated by nonprofit corporations or nonprofit research institutes;
* Government-operated offices, research entities, or national laboratories;
* Government-operated "stealth," "skunk works," "black," or "top secret" research facilities; or

* "Safe houses" disguised as ordinary residential or commercial structures, mobile homes, etc.

The size and layout of suspect facilities to be inspected may range in size from relatively small single-story above-ground brick-and-mortar leased office buildings[23] to a sprawling complex such as the 536,507 ft^2 NIST Advanced Measurement Laboratory Complex[24] in Gaithersburg MD – parts of which are located 40 feet underground and are equipped with extreme vibration isolation,[25] Faraday cage rooms,[26] positive-pressure clean rooms,[27] and the like. Facilities to be inspected may have multiple floors and multiple rooms on each floor, with entry to some rooms requiring passage through multiple hermetically sealed doors.[28] Personnel entry to some labs may be restricted by man traps,[29] and may require special-suited workers to undergo external chemical washes, ultraviolet (UV) irradiation, or electromagnetic pulse (EMP) or similar electronic exposures prior to entry to the facilities. Other suspect facilities may be almost totally automated, seldom requiring human entry and needing only physical inputs of chemical feedstock, electrical power, and instructions in order to manufacture atomically precise product. In the present analysis it is assumed that suspect facilities are protected only by conventional means, and not by more effective means (e.g., military patrol nanorobots) that might someday become available to them through the use of atomically precise manufacturing.

2.2 Inspection Targets

Once the inspection devices have entered a suspect facility pursuant to an authorized inspection mission, they must search for evidence of proscribed APM equipment or activities. In descending order of urgency, the proscribed items and activities include:

Level I. Operating Nanofactories. All legal operating nanofactories must be strictly regulated per Treaty and registered in a master compendium along with their physical location, operating entity or owner, operational and security specifications, and so forth. Any operating nanofactory that is not on the official list is *per se* illegal. Physical tests must be devised that can unambiguously identify an operating nanofactory. Any nanorobotic device that is capable of self-replication, including at highest priority any devices capable of free-range replication or replication using widely-available feedstock materials,[30] is considered to be a "nanofactory".

---

[23] e.g., Molecular Medicine Research Institute, Sunnyvale CA; https://www.mmrx.org/contact/.

[24] NIST Advanced Measurement Laboratory, Gaithersburg MD; https://www.nist.gov/director/pao/advanced-measurement-laboratory.

[25] https://en.wikipedia.org/wiki/Vibration_isolation.
[26] https://en.wikipedia.org/wiki/Faraday_cage.
[27] https://en.wikipedia.org/wiki/Cleanroom.
[28] http://www.dortek.com/door-type/hermetic-doors/.
[29] https://en.wikipedia.org/wiki/Mantrap_(access_control).

[30] e.g., Freitas RA Jr. Some Limits to Global Ecophagy by Biovorous Nanoreplicators, with Public Policy Recommendations. Zyvex Corporation, Apr 2000; http://www.rfreitas.com/Nano/Ecophagy.htm.

Level II. Nanofactories Under Construction. Similarly, all nanofactories that are legally under construction should be of official record, hence any nanofactory under construction that is not on the official permit list is *per se* illegal. Physical tests must be devised that can unambiguously identify a nanofactory under construction. The regulatory mission will succeed even if an inspection approach has difficulty distinguishing between an operating nanofactory and a nanofactory under construction, since both are illegal if unregistered.

Level III. Nanofactory Ramp Intermediates. Nanofactory "ramp" intermediates include static or operating components of an exponential technical developmental ramp of nanomanufacturing capability. This could include components similar to nanofactory development pathways that are known to Treaty signatories who already possess nanofactories and might be employed by others who have directly stolen or copied the technology pathway, or plausible alternative pathways proposed by others involving components that Treaty signatories did not use. Unfamiliar development components and processes might be difficult to reliably recognize in isolation, which suggests that the diagnostic observables of a technical development ramp in progress should also be examined during the facility inspection process. Ramp observables might include direct measurements of exponentially increasing masses or volumes of atomically precise components, exponentially increasing energy generation or cooling requirements in facilities known to possess nanomanufacturing equipment or atomically precise materials, or other observables that may accompany the exponential growth of atomically precise manufacturing facilities.

Level IV. Operating Molecular Workstations.[31] This category is intended to include pre-ramp atomically precise objects that can only be made using APM, along with the scanning probe (or other) equipment that is being used to build these objects. This category would include specific kinds of components combined in a single device that may include an SPM, picometer-level displacement metrology equipment, a continuous source of feedstock needed to fabricate atomically precise objects, and cryogenic ultrahigh vacuum (UHV) environmental control sufficient to enable a continuous atomically precise manufacturing operation to proceed. Inspection devices could also search for evidence of mechanosynthetic processes being executed or for the known byproducts of such processes, including intermediate mechanosynthetically-fabricated partially completed structures.

Level V. Atomically Precise Products. The mere presence of APM products at a facility indicates that they might have been manufactured locally. Purchasing and shipping logs can be consulted *ex post* to determine if the observed APM products have been acquired legally or not. If there is no legal acquisition record, then even if resale of legal APM products and mere possession of APM products is not illegal, the unexpected presence of such products in a facility potentially capable of their manufacture raises suspicion. Searches for atomically precise products are also essential in order to ensure that possible alternative APM technology pathways

---

[31] See, for example: (1) Freitas RA Jr. Molecular Workstation Roadmap I: Survey of Key Technologies Needed to Perform Positionally Controlled Diamondoid Mechanosynthesis using a Molecular Workstation**.** IMM Report No. 59, 2009/2025; http://www.imm.org/Reports/rep059.pdf. (2) Freitas RA Jr. Molecular Workstation Roadmap II: Survey of Single-Atom Tips (SATs) for Diamondoid Mechanosynthesis**.** IMM Report No. 60, 2010/2025; http://www.imm.org/Reports/rep060.pdf. (3) Freitas RA Jr., Merkle RC. A Nanofactory Roadmap: Research Proposal for a Comprehensive Diamondoid Nanofactory Development Program. IMM Report No. 58, 2008/2025; http://www.imm.org/Reports/rep058.pdf.

other than the conventional cryogenic UHV SPM pathway (e.g., biotechnology-based or self-assembly-based pathways) will be detected by the APM Treaty Compliance Inspection Program.

Level VI. Plans, Models, and Simulations. Information including blueprints, designs, models and active simulations of nanofactories and nanofactory-enabling devices and technologies, including molecular workstations, should be actively sought. The discovery of such information, which will not be *per se* illegal in all cases if unregistered, will nonetheless mandate closer inspection of the suspect facility and should elevate the priority level of that inspection.[32] Any specific consideration of means by which products of regulated nanofactories could further aid inspections for these proscribed items outside of research or production facilities is beyond the scope of this document.

Level VII. Key Workstation Enabling Technologies. This is the broadest category of search and as such should be conducted at a much coarser level of completeness, primarily to help rank the facilities already identified above for closer scrutiny according to the probability that they might harbor an unregulated APM operation. Information on all relevant entities, including their location, ownership, and purported activity, should be compiled in a database drawn from publicly and privately available sources, then ranked according to their likely risk of harboring unlawful equipment or activities, based on the number and significance of items of interest that are present at the facility.

Inspections should then be conducted, starting with unregistered facilities deemed to be of highest risk (based on urgency level, prior authorization status, and informed suspicions) and continuing to lower-risk candidates. In descending order of importance, locations of greatest inspection interest in this category will include:

(1) installations where an SPM of any kind is known or suspected to be (or to have been) present,[33] or manufacturers of such equipment;[34]

---

[32] Treaty agreement on if and how to deal with this category may be especially contentious, as it is amenable to classic information technology espionage.

[33] The U.S. SPM market size was estimated at $0.56B (up to 5600 units/yr) in 2021 rising to $0.93B (up to 9300 units/yr) in 2027 (https://www.grandviewresearch.com/industry-analysis/microscopes-industry), assuming ~$100K per high-end microscope that could be usefully incorporated into an atomically precise manufacturing system.

[34] According to this 2021 industry report that costs $4000 to purchase, there are 15 key worldwide manufacturers of scanning probe microscopes (Agilent Technologies; Bruker Nano; Hitachi High-Tech Science Corporation; NT-MDT; Oxford Instruments/Asylum Research; Park Systems; AIST-NT; Anasys Instruments; Anfatec; Angstrom Advanced Inc.; APE research srl; JPK Instruments; Kleindiek Nanotechnik; Multiprobe, Inc; and Nanonics Imaging) that are mostly sold into 15 countries of the world (North America [United States, Canada], Europe [Germany, France, U.K., Italy, Russia], Asia Pacific [China, Japan, South Korea, Taiwan], Southeast Asia [India, Australia], and Latin America [Mexico, Brazil])); https://www.wicz.com/story/43572985/scanning-probe-microscopes-market-size-2021-cagr-value-growth-rate-sales-revenue-latest-trends-top-manufacturers-by-2027.

(2) installations where sub-Angstrom or picometer-scale displacement metrology research or development activities are known or suspected to be (or to have been) underway, or manufacturers of such equipment;

(3) laboratories or institutions that are mentioned in (or which employ personnel listed as authors or in the acknowledgements section of) technical papers, books, book chapters, web sites, conference presentations, patents, or videos describing: (A) positionally controlled chemistry, (B) positionally controlled fabrication or assembly, (C) mechanosynthesis, (D) nanomechanical research, (E) nanofactories or nanorobotics, (F) atomically sharp, single-crystal, or single-atom SPM tips, or (G) any form of APM research, APM fabrication, or APM manufacturing work, whether theoretical or experimental;

(4) installations using any form of UHV chamber for any purpose, or manufacturers of such equipment;

(5) any facility that regularly purchases or uses any form of cryogenic equipment, including all users of LN2 and LHe; and

(6) any facility that regularly purchases or uses any form of germanium or organogermanium compounds.[35]

Results of inspections of suspect facilities are reported back to the APM Treaty Compliance Inspection Program authority for further action.

The inspection mission "regime" should include testing of mission scenario elements and mission scenarios on representative test installations, and should incorporate feedback from tests and real missions to improve the design and operation of all Treaty Compliance inspection operations.

2.3 Inspection Timeframes

The speed with which unregulated facilities must be detected and reported is a key operational and design parameter that needs more explicit analysis. It is generally believed, based on past experience, that progress from SPM and Molecular Workstations to a working nanofactory is very time-consuming and labor-intensive, but that once a nanofactory exists which is capable of at least milligram/day manufacture of atomically precise product, the risk of potentially disruptive activities rises exponentially – especially if nanofactory production capacity is also increasing exponentially.

For illegal Level I facilities (i.e., operating nanofactories) – the highest level of urgency – the appropriate response time for Treaty compliance inspections is on the order of a few multiples of the estimated net replication time of the nanofactory. For example, if an operating nanofactory is

---

[35] This highly specific item is included solely because of the key role played by germanium in proposed schemes for implementing practical diamondoid mechanosynthesis, e.g., Freitas RA Jr., Merkle RC. A minimal toolset for positional diamond mechanosynthesis. J Comput Theor Nanosci. 2008;5:760-861; http://www.molecularassembler.com/Papers/MinToolset.pdf.

doubling its manufacturing capacity every ~1 week, then inspections should be conducted and concluded in a time frame on the order of a few weeks.

For illegal Level II facilities (i.e., nanofactories under construction), an estimate should be made of the likely breakout time until the facility is expected to reach gram/day atomically precise output capacity. In this case, the maximum response time for concluding a Treaty compliance inspection is on the order of the likely breakout time. For illegal lower-Level items, more time may be allowed before the conclusion of necessary Treaty compliance inspections.

How much inspection-oriented atomically precise machinery must be manufacturable and operable by the APM Treaty Compliance Inspection authority in order to maintain the inspection regime proposed in this document? Assuming ~10,000 SPMs capable of being usefully incorporated into an atomically precise manufacturing system are sold annually worldwide, each with a working lifetime of ~10 years, and if at least 5 SPMs are required in a development facility to undertake a credible nanofactory development program, there may be up to 20,000 facilities worldwide needing Treaty-related inspections. If the floor space of each of these facilities averages ~5000 ft^2 (a reasonable minimum requirement for such development work), then each Delivery Drone must carry approximately (5000 ft^2) (~1 liter / 500,000 ft^2) ~ 10 cm^3 ~ 20 gm of inspection nanorobots (Section 3.7). Inspecting each of the 20,000 facilities once a year assuming 36.5 days per inspection cycle would then demand at least [(36.5 days) / (365 days/year)] (20,000 facilities/year) (20 gm of nanorobots / facility) ~ **40 kg of inspection nanorobots** and (20,000 inspections/year) / (10 inspections/drone-year) ~ **2000 Delivery Drones** to operate the Treaty compliance inspection regime. The actual required inspection nanorobot mass could be tenfold higher, or more, and may be estimated more precisely after the first list of potential target facilities has been compiled.

If the more typical inspection event requires on the order of some tens of grams of inspection nanorobots, this implies that it may be possible to launch at least some inspection capability even using early-generation lower-productivity nanofactories that are owned and legally operated by the Treaty monitoring authority.

The response to a detected illegal activity may require larger masses of nanomachinery but is beyond the scope of this document.

3. Nanofactory-Enabled Inspection Devices and Tasks

In addition to well-known conventional means of data collection, nanorobots represent a uniquely effective class of inspection instrumentality. Nanorobots may be so small as to be invisible to the human eye or to other common means of detection. Their entry into facilities and subsequent inspection thereof cannot easily be curtailed without employing defensive systems using a similar level of advanced machine-phase nanotechnology – **which this document presumes will not yet be available to the suspect facilities under investigation**, provided that the Treaty authorities establish and maintain their "first mover" persistent technological advantage. Nanorobots can only be manufactured in nanofactories, and the purpose of the APM Treaty is to prevent unregulated entities (A) from gaining access to nanofactories or (B) from manufacturing unregulated APM nanodevices.

Nanorobotic inspection devices will have basic limitations on size (Section 3.1) and power (Section 3.2), stemming from the need for stealth operation. After compiling a comprehensive map of the suspect facility (Section 3.3), inspection nanorobots can search the premises for a variety of observables that may be used to infer, prove, or disprove a potential Treaty violation. Such observables may be of two basic types: unconcealed observables (Section 3.4) and concealed observables (Section 3.5). Different nanorobotic instrumentalities are required to collect these two kinds of data. If a nanorobot suffers some kind of mechanical failure or is detected by suspect facility personnel, optional protocols for automatic self-destruction should be available for inspection nanodevices to use (Section 3.6). Transportation of inspection nanorobots to and from the suspect facility may be accomplished using a Delivery Drone (Section 3.7).

3.1 Inspection Device Size

Because an important security advantage is that the presence of inspection robots should not be obvious to casual human observers who might seek to defeat their purpose,[36] the upper limit on robot size should normally be just below the lower limit of human visual acuity at maximum contrast (e.g., black particles against a solid white background).[37] Normal "20/20" or "6/6" acuity corresponds to distinguishing black-on-white contours 1.75 mm apart at a distance of 6 meters,[38] or about 1 minute of arc. If the minimum distance that a human eye can focus (i.e., the maximum accommodation distance)[39] is d_{accomm} = 6.5 cm from the eye of a young person, then the minimum distinguishable size would be (6.5 cm / 6 m) (1750 μm) = **19 μm**.

The resolution of the human eye is constrained by the diffraction limit[40] which can be approximated by $\theta_{object} \approx 1.22\ \lambda_{light} / D_{pupil}$ = 1.2-4.3 x 10^{-4} rad = 0.41-1.5 arcmin, where θ_{object} is the angular size of the object under scrutiny, the wavelength of visible light is λ_{light} = 400-700 nm, and the diameter of the human eye pupil aperture (as regulated by the iris) under normal daytime lighting conditions is D_{pupil} = 2-4 mm.[41] This corresponds to a minimum visible object size of $x_{visible} = d_{accomm}\ \theta_{object}$ = **8-28 μm** (at 400-700 nm wavelengths) for a young child with excellent visual acuity with d_{accomm} = 6.5 cm, or $x_{visible}$ = **30-108 μm** for normal adult eyes with d_{accomm} = 25 cm for comfortable viewing.[42] Also note that incoming light must strike two separate cone cells in the human eye in order for the brain to register separate pixels; cones in the densest center of the fovea centralis are spaced about x_{cone} = 2 μm apart[43] and the diameter of the human eye in the front-to-back direction is $D_{eyeball}$ ~ 24 mm,[44] hence by simple geometry θ_{object} ~

---

[36] Commonplace automated area-coverage security cameras with a square 3-meter field of view and 8.3 megapixel (UHDTV or 4K; https://en.wikipedia.org/wiki/Ultra-high-definition_television) resolution provide ~1 mm^2 pixels. A $(20\ \mu m)^2$ pixel size would require a ~23 gigapixel camera to cover a 3 m x 3 m field of view. In 2013, DARPA unveiled a 1.8 gigapixel military drone camera (https://www.extremetech.com/extreme/146909-darpa-shows-off-1-8-gigapixel-surveillance-drone-can-spot-a-terrorist-from-20000-feet), and the Large Synoptic Survey Telescope (completion expected in 2023) has the world's largest digital camera at 3.2 gigapixels and ~2800 kg (https://www.lsst.org/about/camera). Visual security monitoring at 20 μm resolution of a suspect laboratory without the benefit of nanofactory-enabled nanodevices would likely require impractically bulky and expensive cameras that would in any case be immediately recognizable to inspection nanorobots.

[37] Typical household dust mites, due to their small size (200-300 μm in length) and translucent bodies, are barely visible to the unaided human eye; https://en.wikipedia.org/wiki/House_dust_mite.

[38] https://en.wikipedia.org/wiki/Visual_acuity#Definition.
[39] https://en.wikipedia.org/wiki/Accommodation_(vertebrate_eye)
[40] https://en.wikipedia.org/wiki/Angular_resolution#The_Rayleigh_criterion.
[41] https://en.wikipedia.org/wiki/Pupil#Effect_of_light.
[42] https://www.quora.com/Vision-eyesight-What-is-the-smallest-thing-a-human-eye-can-see-and-why.
[43] https://en.wikipedia.org/wiki/Fovea_centralis.
[44] https://en.wikipedia.org/wiki/Human_eye#Size.

$x_{cone} / D_{eyeball} = 8.3 \times 10^{-5}$ rad, giving $x_{visible} = d_{accomm}\ \theta_{object}$ = **21 µm** for normal adult eyes with d_{accomm} ~ 25 cm (at age 45)[45] in normal daytime lighting conditions.

Of course, dark-adapted rod cells in human eyes can detect individual photons of light,[46] and the naked human eye can see objects of any size that glow (emit light),[47] or objects as small as **10 µm** that scatter enough light (e.g., bubbles or transparent particles that scatter sunlight)[48] to trigger the eye's detector cells. Notes one author: "Light visible from the star Deneb covers a minuscule fraction of your visual field (its 'angular diameter' is 0.0024 arcsec – a light-emitting object, seen as the same size when 15 cm from your face, would be 1.75 nanometers wide. What is limited is the eye's resolution: how close two objects can become before they blur into one. At absolute best, humans can resolve two lines about 0.01 degrees apart: a **26 µm** gap, if positioned 15 cm from your face. In practice, objects **40 µm** wide (the width of a fine human hair) are just distinguishable by good eyes; objects **20 µm** wide are not." [49] Thus inspection nanorobots that are intended to remain nearly invisible to the human eye should not have reflective or light-scattering surfaces and should not emit photons in the visible portion of the spectrum.

These considerations suggest that an **inspection nanorobot** should be no larger than ~**20 µm** in any dimension and should not have high visual contrast relative to its surroundings if it is attempting to appear "invisible" to human eyes under normal daytime lighting conditions. A robot about 20 µm in size would be at or below the limit of what the average human eye can detect under normal conditions.

Very long thin nanorobot shapes might become visible to the human eye in certain circumstances, even if they are smaller than the ~20 µm limit of human eye resolution. For example, vernier acuity, aka. hyperacuity,[50] is that ability of the human eye to align two visible line segments. Under optimal conditions of good illumination, high contrast, and long line segments, the limit to vernier acuity is about 0.13 arcmin (~**9 µm** at 25 cm viewing distance).[51] Similarly, the smallest detectable visual angle produced by a single fine dark line against a uniformly illuminated

---

[45] Duane A. Studies in Monocular and Binocular Accommodation, with Their Clinical Application. Trans Am Ophthalmol Soc. 1922;20:132-57; https://pmc.ncbi.nlm.nih.gov/articles/PMC1318318/pdf/taos00079-0136.pdf.

[46] Tinsley JN, Molodtsov MI, Prevedel R, Wartmann D, Espigulé-Pons J, Lauwers M, Vaziri A. Direct detection of a single photon by humans. Nat Commun. 2016 Jul 19;7:12172; https://www.ncbi.nlm.nih.gov/pmc/articles/PMC4960318/. See also: https://www.nature.com/news/people-can-sense-single-photons-1.20282.

[47] The human brain will only register a detection event 4-10 times out of 100 photon impacts on a photoreceptor cell. https://www.quora.com/Vision-eyesight-What-is-the-smallest-thing-a-human-eye-can-see-and-why and http://math.ucr.edu/home/baez/physics/Quantum/see_a_photon.html.

[48] "How Small of a Particle Can We See?" 28 Feb 2014; https://web.archive.org/web/20200410212153/https://www.me.psu.edu/cimbala/me405/Lectures/Slides_Particles.pdf.

[49] https://www.sciencefocus.com/the-human-body/how-small-can-the-naked-eye-see/.
[50] https://en.wikipedia.org/wiki/Hyperacuity_(scientific_term).
[51] https://en.wikipedia.org/wiki/Visual_acuity#Other_measures.

background is also much less than foveal cone size or regular visual acuity, with a limit of ~0.5 arcsec (2.4×10^{-6} rad, or ~0.6 μm at a 25 cm viewing distance) or only about 2% of the diameter of a foveal cone, producing a contrast of about 1% with the illumination of surrounding cones. The mechanism of detection is the ability to detect such small differences in contrast or illumination and does not depend on the angular width of the bar, which cannot be discerned. Thus as the line gets finer, it appears to get fainter but not thinner.[52] Another unresolved question is whether a non-reflective and non-glowing nanorobot whose width was smaller than the shortest wavelength of visible light (e.g., ≤ 200-400 nm) but was extremely long in another dimension could be visible to the human eye. Further experimental research on these issues is warranted.

One final consideration is the existence of separate visual acuity limits for otherwise visible objects that are in lateral motion across the field of view. In one experiment,[53] moving objects were foveally detected when they displaced 0.68 arcmin (near the human visual limit) at an angular velocity of $\theta_v \geq 0.001$ rad/sec, implying a maximum velocity limit on the locomotion of nanorobots seeking to remain unnoticed of $v_{visible} = d_{accomm}\ \theta_v =$ **0.25 mm/sec** at the closest viewing distance of $d_{accomm} = 25$ cm for normal adults. As another example, visual fixation[54] on a scene is interrupted by frequent saccades of the human eye, and a saccade in response to an unexpected stimulus normally takes $t_{initsac} \sim 200$ ms to initiate.[55] If object motion must be detected during the period of pre-saccade fixation, then an $x_{visible} = 20$ μm motion at a viewing distance of $d_{accomm} = 25$ cm represents a $\theta_{object} = x_{visible} / d_{accomm} = 8 \times 10^{-5}$ rad angular displacement, giving an angular velocity of $\theta_v = \theta_{object} / t_{initsac} = 4 \times 10^{-4}$ rad/sec during the 200 ms period of pre-saccade fixation and $v_{visible} = d_{accomm}\ \theta_v = x_{visible} / t_{initsac} =$ **0.10 mm/sec** at the closest viewing distance of $d_{accomm} = 25$ cm for normal adults. Further research is needed to confirm whether nanorobots with static invisibility might become visible when they move too fast.

Compliance Program nanorobot designers might also consider a camouflage or fauna mimicry mission profile[56] to allow using larger nanorobots, depending on the local culture and physical environment.

---

[52] https://en.wikipedia.org/wiki/Visual_acuity#Other_measures.

[53] Lappin JS, Tadin D, Nyquist JB, Corn AL. Spatial and temporal limits of motion perception across variations in speed, eccentricity, and low vision. J Vis. 2009 Jan 22;9(1):30.1-14; https://jov.arvojournals.org/arvo/content_public/journal/jov/932855/jov-9-1-30.pdf.

[54] https://en.wikipedia.org/wiki/Fixation_(visual).

[55] https://en.wikipedia.org/wiki/Saccade#Timing_and_kinematics.

[56] Matthews R, Matthews TJ. Military mimicry: the art of concealment, deception, and imitation. Defense & Security Analysis 2024;40(3):379-404; https://www.tandfonline.com/doi/full/10.1080/14751798.2024.2352271.

3.2 Inspection Device Power

Nanorobotic inspection devices will be limited in their range of actions by the availability of onboard power.

The greatest freedom of action is obtained when the source of energy is entirely internal to the nanorobot (e.g., an onboard battery), but using only an internal source means that the total available energy is finite and robot activities must terminate when the onboard supply is exhausted. Convenient internal power supplies for nanorobots might include chemical batteries, fuel cells, nonambient combustion, mechanical springs or flywheels, or radioisotope decay.

Energy can also be absorbed from the environment (e.g., a photovoltaic cell) and buffered using an onboard storage device, providing a potentially unlimited supply of power. But using only external sources means that robot activities will be limited in duration to the capacity of the onboard buffer if access to the environmental supply is cut off (e.g., room lighting is turned off or the robot enters a dark vacuum chamber, in the case of photovoltaic external power). Convenient external power supplies for nanorobots may include photovoltaic cells, ambient combustion (i.e., onboard fuel with oxygen drawn from the air), ambient radio or microwave radiation, electrical energy tapped directly from 60 Hz/110 VAC wall outlets or indirectly from poorly shielded electric motors or cables attached to operating electric-powered equipment, and acoustic vibrations carried through available solid, liquid or gaseous media.

3.2.1 Power Sources

A conservative estimate of the energy and power densities potentially available to nanorobots from each of these sources includes:

* **Chemical Battery.** A lithium-fluorine battery would have the highest known theoretical energy density (E_D ~ 25.1 MJ/L) if it could be built.[57] One of the highest energy density batteries demonstrated experimentally to date is the lithium-carbon monofluoride battery at 5.32 MJ/L, though with a power density of only P_D ~ 0.000152 MW/L.[58] Rechargeable lithium-ion polymer batteries[59] –commonly used in radio-controlled aircraft, cars, helicopters and drones – are available commercially with an energy density of 1 MJ/L from TrakPower[60] or 2

---

[57] Freitas RA Jr. Energy Density. IMM Report No. 50, 25 June 2019, Section 4.1.1 Electrochemical Batteries; http://www.imm.org/Reports/rep050.pdf.

[58] De-Leon S. Li/CFx Batteries: The Renaissance. Shmuel De-Leon Energy, Ltd, 6 Aug 2011; https://www.sdle.co.il/wp-content/uploads/2018/08/li-cfx-the-renaissance.pdf.

[59] https://en.wikipedia.org/wiki/Lithium_polymer_battery. "Test reports warn of the risk of fire when the batteries are not used in accordance with the instructions."

[60] e.g., "TrakPower LiPo 2S 7.4V 4000mAh 50C Hard Case 4mm Short" (https://www.towerhobbies.com/cgi-bin/wti0001p?I=LXHHAW&P=SM) battery pack, featuring 30 Wh (108,000 J) capacity in a 47 x 24 x 96 mm (108,288 mm^3) volume.

MJ/L from Amicell.[61] Innolith AG claims to have a 3.6 MJ/kg rechargeable lithium-ion battery,[62] and rechargeable thin-film lithium-ion batteries may have the potential to reach 3.6 MJ/L.[63]

* **Fuel Cell.** A hydrogen-oxygen fuel cell could theoretically achieve $E_D \sim 5.57$ MJ/L if both reactants could be pressurized to near-liquid densities.[64] The highest-capacity commercially-available fuel cell currently achieves $E_D \sim 1.36$ MJ/L.[65] Fuel cells generally have a good energy density but poor power density, typically no higher than $P_D \sim 0.02$ MW/L, though it has been speculated that nanoscale fuel cell power densities in the range of $P_D \sim 700$ MW/L might be possible using atomically precise structures fabricated in nanofactories.[66]

* **Nonambient Combustion.** In nonambient combustion, both fuel and oxidant are contained entirely within the energy storage system. Theoretically, the combustion of beryllium metal and fluorine compressed to near-liquid density would achieve $E_D \sim 41.7$ MJ/L, or $E_D \sim 31.7$ MJ/L using liquid-density oxygen. The most stable organic fuel is kerosene, which when burned in oxygen achieves $E_D \sim 12.4$ MJ/L.[67] In all cases, the generated combustion heat must be converted to useful mechanical or electrical energy with substantial unavoidable loss of energy efficiency.

* **Mechanical Spring.** Twisted carbon nanotubes may store up to $E_D \sim 8.8$ MJ/L of mechanical torsion energy,[68] but working storage systems will achieve less than this due to the need for mechanical infrastructure surrounding the twisted nanotubes.

---

[61] Extreme high energy density Lithium Polymer series, ABLPA655275HG (https://www.amicell.co.il/batteries/rechargeable-batteries/our-extreme-high-energy-density-lithium-polymer-series/) lithium power cell, featuring 23.88 amp-hour at 3.7 volt (318,082 J) capacity in a 10.6 x 55 x 271 mm (157,993 mm^3) volume.

[62] Bryony Collins, "Innolith Battery Strikes at 'Flammable' Lithium-Ion: Q&A," BloombergNEF, 13 May 2019; https://about.bnef.com/blog/innolith-battery-strikes-flammable-lithium-ion-qa/.

[63] https://web.archive.org/web/20120912092549/http://www.excellatron.com/advantage.htm.

[64] Freitas RA Jr. Energy Density. IMM Report No. 50, 25 June 2019, Section 4.1.2 Fuel Cells; http://www.imm.org/Reports/rep050.pdf.

[65] "Smart Fuel Cell Jenny 1200 50W DMFC fuel cell (Direct Methane Fuel Cell)," http://www.sfc-defense.com/sites/default/files/160530_produktdatenblatt_jenny_1200_en_online.pdf. Data: 4.32 MJ charging capacity/day = 50 W; 50 W x 100 hr x 3600 sec/hr = 18 MJ; mass = 7.6 kg, volume = 13.24 L; therefore 2.37 MJ/kg, 1.36 MJ/L, 6.58 W/kg, 3.78 W/L.

[66] Freitas RA Jr. Energy Density. IMM Report No. 50, 25 June 2019, Section 4.1.2 Fuel Cells; http://www.imm.org/Reports/rep050.pdf.

[67] Freitas RA Jr. Energy Density. IMM Report No. 50, 25 June 2019, Table 28. Energy density of fuel-oxidant materials during nonambient combustion; http://www.imm.org/Reports/rep050.pdf.

[68] Freitas RA Jr. Energy Density. IMM Report No. 50, 25 June 2019, Section 5.2 Springs; http://www.imm.org/Reports/rep050.pdf.

* **Flywheel.** The theoretical maximum energy density for a constant-stress solid disk flywheel made of defect-free diamond crystal, spinning at near-bursting speed and riding on a single-atom acetylenic rotary joint is $E_D \sim 90$ MJ/L.[69] Further analysis is needed to determine if coupling to the rotational energy, either to extract the energy or to re-spin a discharged rotor, might be technically challenging or could involve significant loss of energy efficiency given the infrastructure required.

* **Radioisotope Decay**. Most high-energy radioisotopes are short-lived and emit harmful radiation that may be detectable via Geiger counter[70] in some facilities. Among radioisotopes with a half-life exceeding 1 year, ^{208}Po may be the most readily available and emits only α and β^+ particles which can be mostly shielded inside microscale containers and converted to electrical power, achieving energy density of $E_D \sim 2.22 \times 10^7$ MJ/L with a power density of $P_D \sim 0.17$ MW/L over a half-life of 2.9 years. ^{238}Pu is the longest-lived naturally occurring pure alpha-emitter and is commonly used in radioisotope thermoelectric generators, with an energy density of $E_D \sim 4.49 \times 10^7$ MJ/L but a power density of only $P_D \sim 0.0112$ MW/L over a half-life of 87.8 years.[71]

* **Photovoltaic Cell.** Photovoltaic cells capable of converting ambient visible light into electricity are available commercially with efficiency up to $\varepsilon_{photo} \sim 20\%$,[72] and by 2025 research systems had demonstrated 47.6% efficiency,[73] with theoretical efficiencies up to 85% if concentrators, nantennas, and other tricks are used.[74] If the average illumination typically available inside well-lighted buildings (when the lights are on) is $I_{lab} \sim 10$ W/m^2,[75] then a nanorobot surface coated with $\varepsilon_{photo} = 20\%$ efficient photocells could absorb and convert light to electricity at a delivered power intensity of $I_{photo} \sim \varepsilon_{photo}\, I_{lab} = 2$ W/m^2 = 2 pW/μm^2. If the photocells must be at least as thick as the wavelength of light ($\lambda_{light} \sim$ 400-700 nm), the power density becomes $P_D \sim I_{photo} / \lambda_{light} = 3$-5 pW/μm^3. This energy could be used immediately for

---

[69] Freitas RA Jr. Energy Density. IMM Report No. 50, 25 June 2019, Section 5.3.2 Rotational Motion; http://www.imm.org/Reports/rep050.pdf.

[70] https://en.wikipedia.org/wiki/Geiger_counter.

[71] Freitas RA Jr. Energy Density. IMM Report No. 50, 25 June 2019, Table 51. Energy density (E_D) of α-emitting radionuclides with half-life ≥ 1 day and Table 53. Power density (E_D) of α-emitting radionuclides with half-life ≥ 1 day; http://www.imm.org/Reports/rep050.pdf.

[72] https://news.energysage.com/what-are-the-most-efficient-solar-panels-on-the-market/.
[73] https://en.wikipedia.org/wiki/Solar-cell_efficiency.

[74] Corkish R, Green MA, Puzzer T. Solar energy collection by antennas. Solar Energy 2002;73(6):395-401; https://www.univie.ac.at/photovoltaik/vorlesung/ss2013/unit4/solar_antenna.pdf. Johnson RC. Solar Cells Made Obsolete: 3D rectennas aim at 40%-90% efficiency. EE Times, 28 Sep 2015; https://www.eetimes.com/document.asp?doc_id=1327819. See also: https://en.wikipedia.org/wiki/Optical_rectenna.

[75] "Lighting System Assessment Guidelines," U.S. Dept. of Energy, NREL/BR-7A20-50125, Jun 2011; https://www.nrel.gov/docs/fy11osti/50125.pdf.

operations, or could be stored in one of the forms previously described (e.g., a battery) for use when no ambient illumination is available.

* **Ambient Combustion.** In ambient combustion, the fuel is contained entirely within the energy storage system and the oxidant (typically oxygen) is absorbed from the air. This eliminates the volume requirement for carrying onboard oxidant, but restricts the operation of the system to environments where air is present. The combustion of boron with oxygen compressed to near-liquid density would achieve E_D ~ 271.4 MJ/L, the highest of any known chemical system.[76] Convenient alternatives also employing oxygen combustion include the smallest possible fullerene[77] C_{20} at E_D ~ 145.3 MJ/L and diamond at E_D ~ 115.6 MJ/L. In all cases, the generated combustion heat must be converted to useful mechanical or electrical energy with substantial unavoidable loss of energy efficiency.

* **Ambient Radio or Microwave Radiation**. Radio frequency ambient radiation is typically 0.0024 W/m^2 in city areas with occasional peak readings as high as 0.1 W/m^2,[78] more than 100-fold less intense than ambient visible light. The maximum legally-allowable leakage from an operating microwave oven is 50 W/m^2 at a distance of 5 cm from the oven surface,[79] but this source is sporadic and unlikely to exist in most suspect facilities requiring inspection.

* **Electrical Energy Tap.** Almost every facility is likely to have electrical outlets located periodically along walls and floors, into which electrically-driven equipment can be plugged to obtain power.[80] Abundant power should be available from this source, which should be ubiquitous in virtually all suspect facilities and would include 110/220 VAC voltages, 50/60 Hz alternating current, and two- or three-prong outlets. Double-walled carbon nanotube conductors ~1.6 nm diameter can likely carry ~10 x 10^{-6} amp/wire at 1 volt – consistent with experimental observations[81] of individual 10-50 nm long single-walled "metallic" carbon nanotubes conducting 25-100 x 10^{-6} amp/wire electrical currents before failing, along with a peak burnout threshold of ~1000 x 10^{-6} amp/wire as reported by others.[82] Extending a ~1.6 nm

---

[76] Freitas RA Jr. Energy Density. IMM Report No. 50, 25 June 2019, Section 4.2.3 Ambient Chemical Combustion; http://www.imm.org/Reports/rep050.pdf.

[77] Lin F, Sorensen ES, Kallin C, Berlinsky AJ. Chapter 29. C_{20}, the Smallest Fullerene. Handbook of Nanophysics: Clusters and Fullerenes, 2009, pp. 29-1 – 29-11; http://www1.phys.vt.edu/~feilin/papers/C20chapter.pdf.

[78] Hedendahl LK, Carlberg M, Koppel T, Hardell L. Measurements of radiofrequency radiation with a body-borne exposimeter in Swedish schools with Wi-Fi. Front. Public Health 2017 Nov 20; https://www.frontiersin.org/articles/10.3389/fpubh.2017.00279/full.

[79] https://en.wikipedia.org/wiki/Microwave_oven.
[80] https://en.wikipedia.org/wiki/AC_power_plugs_and_sockets.

[81] Javey A, Qi P, Wang Q, Dai H. Ten- to 50-nm-long quasi-ballistic carbon nanotube devices obtained without complex lithography. PNAS 2004 Sep 14;101:13408-13410; http://www.pnas.org/cgi/content/abstract/101/37/13408.

[82] Dai H, Wong EW, Lieber CM. Probing Electrical Transport in Nanomaterials: Conductivity of Individual Carbon Nanotubes. Science 1996 Apr 26;272:523-526;

diameter nanotube conductor across the 4 mm separation between adjacent conductors in standard 15-amp Romex[83] wire requires the nanorobot to furl and unfurl a negligible ~0.008 μm^3 volume of nanotube, so we can reasonably assume that a ~100 μm^3 mechanical extension/retraction and electrical recharging system volume should suffice. The power draw at 10 x 10^{-6} amp/wire and 1 volt is 1 x 10^{-5} W, enough to recharge a large nanorobot in seconds (see below). Coax connections, USB ports, light bulb sockets, computer circuits, electric motors, and the like are also available for direct electrical tapping. Indirect tapping of stray electromagnetic fields caused by the movement of current through conductors, as with ambient radio, may be much less useful for power generation. For instance, the magnetic field a distance d_{wire} = 10 μm from a long straight wire carrying alternating current of i_{wire} = 10 amps is approximated[84] by Ampere's Law as $B = \mu_0 \, i_{wire} / 2 \, \pi \, d_{wire}$ = 0.2 tesla, using permeability constant μ_0 = 1.26 x 10^{-6} henry/meter, which would provide a local energy density of only $E_D = B^2 / 2 \, \mu_0$ = 1.6 x 10^{-5} MJ/L = 0.016 $pJ/\mu m^3$.

* **Acoustic Vibration.** A previous analysis[85] suggests that air pressure changes from people talking (ΔP_{sound} ~ 0.005 atm) or shouting (ΔP_{sound} ~ 0.05 atm) at a υ_{sound} = 1000 Hz frequency can be converted to mechanical power producing a power density of at most $P_D \leq \Delta P_{sound} \, \upsilon_{sound}$ = 0.005 MJ/L = 5 $pJ/\mu m^3$. Footfall impacts can produce pressure spikes of ~0.4 atm at ~1 Hz on solid floors,[86] which is even less energetic. Except for extremely noisy laboratories, usable sources of acoustic power are likely to be sporadic and rare.

No single power source is ideal, so a multimodal approach is proposed in Section 3.2.2 to harness the best aspects of several sources.

3.2.2 Multimode Power System Configuration

To maximize both freedom and duration of action while maintaining high reliability through redundancy, a reasonable nanorobot design might employ five separate but interconnected power systems:

(1) a rechargeable lithium-ion **electric battery** for continuous operating power and primary onboard energy buffer storage (E_D ~ 3 MJ/L for an entire cell);

---

http://www.academia.edu/download/24927806/science272_523.pdf. Frank S, Poncharal P, Wang ZL, de Heer WA. Carbon Nanotube Quantum Resistors. Science 1998 Jun 12;280:1744-1746; http://www.nanoscience.gatech.edu/paper/1998/98_sci_1.pdf.

[83] https://en.wikipedia.org/wiki/Thermoplastic-sheathed_cable#North_America.
[84] https://www.physicsforums.com/threads/b-field-of-a-wire-carrying-ac-current.512203/.

[85] Freitas RA Jr., Nanomedicine, Volume I: Basic Capabilities, Landes Bioscience, Georgetown, TX, 1999, Section 6.3.3 Acoustic Energy Conversion Processes; http://www.nanomedicine.com/NMI/6.3.3.htm.

[86] Freitas RA Jr., Nanomedicine, Volume I: Basic Capabilities, Landes Bioscience, Georgetown, TX, 1999, Table 6.3; http://www.nanomedicine.com/NMI/Tables/6.3.jpg.

(2) **mechanical springs** for brief burst power (E_D ~ 3 MJ/L for an entire mechanical system);

(3) **electrical energy taps** for primary energy resupply (P_{tap} ~ 1 x 10^{-5} W per ~100 μm^3 of robot volume for an entire recharge mechanism);

(4) **photovoltaics** for secondary (backup) energy resupply (I_{photo} ~ 2 pW/μm^2 and $P_{D,photo}$ ~ 2 pW/μm^3 for an entire cell system); and

(5) **battery relay shuttles** from the Drone to support occasional large-energy operations.

As a simple scaling exercise, consider an exemplar cube-shaped inspection nanorobot with maximum ("invisible") size L_{robot} = **20 µm**, volume $V_{robot} = L_{robot}^3$ = 8000 μm^3, and $f_{storage}$ = 10% of robot volume allocated to some optimal combination of battery (continuous) and mechanical (burst) energy storage, or $V_{storage} = f_{storage}\ V_{robot}$ = 800 μm^3, giving the robot $E_{robot} = E_D\ V_{storage}$ = **2.4 x 10^6 pJ** of combined battery and burst energy to draw upon, taking E_D ~ 3 MJ/L. This is enough to provide **1000 pW of continuous power for 2400 sec** (~40 min).[87] A ~100 μm^3 electrical energy tap **primary recharge system** permits the entire onboard energy store to be recharged in $t_{recharge,tap} \sim E_{robot} / P_{tap}$ = **0.24 sec**, which does not include the time needed to enter the electrical receptacle, locate the appropriate wires within it, extend the taps, then later retract the taps and exit the receptacle, all of which could require several minutes.[88] The **photovoltaic system** can provide continuous recharge power by coating at least all of one cube face with photovoltaic cells, covering $A_{voltaic} = L_{robot}^2$ = 400 μm^2 of robot surface and occupying an additional $V_{voltaic} = (I_{photo} / P_{D,photo})\ A_{voltaic}$ = 400 μm^3, or $f_{voltaic} = V_{voltaic} / V_{robot}$ = 5% of robot volume, producing up to $P_{voltaic} = I_{photo}\ A_{voltaic}$ = 400 pW of continuous power under typical indoor illumination – sufficient by itself to power many normal robot activities (including flight, see below) and enough to recharge the entire onboard energy store in $t_{recharge,photo} \sim E_{robot} / P_{voltaic}$ = 6000 sec (~**1.7 hours**).

Except for fully-automated unmanned facilities, almost all laboratories of interest for inspection will have regular human traffic. Residential, commercial, and even laboratory facilities with clean rooms usually have access doors with sufficiently large gaps in the physical structure to allow a 20 µm object to easily pass. Entry by an inspection nanorobot into a hermetically-sealed[89] facility from the outside, and ingress and egress through similar doorways within the

---

[87] If this duration is deemed insufficient for the inspection mission, a flywheel battery potentially could provide at least 10 times longer operating times than an electric battery, given its much higher theoretical energy density.

[88] This "connection time" overhead along with most of the 100 μm^3 of recharge system structure can be virtually eliminated by deploying specialized nanorobots whose sole task is to enter a room, locate a receptacle, then plug into the room's wiring for the duration of the mission, allowing other robots to use this now-sessile receptacle robot as a convenient fixed-position charging station (e.g., https://en.wikipedia.org/wiki/Tesla_Supercharger) to which they can quickly connect and disconnect. After the mission is completed, receptacle robots can disconnect from the lab wiring and exit the premises with the other robots. Establishing a local network of nanorobotic mobile charging stations would further reduce the mean time to recharge for the primary inspection nanorobots.

[89] http://www.dortek.com/door-type/hermetic-doors/.

facility, is achieved by simply waiting near an entrance for a human to come by, then temporarily and insensibly affixing to the human on their clothing or skin as they pass through the opening, thus minimizing the chances of visual or other sensory detection. At slightly higher risk of visual detection, the nanorobot might crawl or fly through the temporarily open doorway. Conventional security systems will not detect or deter these intrusions because such systems don't screen for the presence of micron-scale robots (or similar microparticles) on arriving or departing personnel for the simple reason that such devices are not yet in common use.

A ~10 μm cubical nanorobot[90] still in the viscous flight regime may burn 5 pW at hover and P_{flight} ~ 350 pW at an airspeed of v_{flight} = 10 cm/sec,[91] a velocity that gives a flying robot with E_{robot} = 2.4 x 10^6 pJ a **maximum flight range** of $X_{flight} = (E_{robot} / P_{flight}) v_{flight}$ = **686 meters** before the energy store would be exhausted and require recharge.[92] A nanorobot with multiple legs ~0.2 μm in length can crawl along flat surfaces at a power cost of P_{crawl} ~ 10 pW with a ground speed of v_{crawl} ~ 1 cm/sec,[93] giving the nanorobot a **maximum crawl range** of $X_{crawl} = (E_{robot} / P_{crawl}) v_{crawl}$ = **2400 meters** using the energy store alone. This allows plenty of capacity for inspection nanorobots to initiate a comprehensive mapping of the facility, since electrical taps and photovoltaics provide unlimited opportunities for recharge of the energy store. Robots can also hitchhike on the clothing or bodies of unknowing personnel (Section 3.4.2), traveling arbitrarily deep into the facility at a negligible cost of onboard energy.

---

[90] Note that a long cylindrical robot feels more viscous resistance to motion through a fluid such as air or water than a more compact (e.g., spherical-shaped) robot when the device is translating normal to its axis, since the cylindrical object has much more surface area per unit volume than a sphere. Freitas RA Jr., Nanomedicine, Volume I: Basic Capabilities, Landes Bioscience, Georgetown, TX, 1999, Section 9.4.2.4 Force and Power Requirements; http://www.nanomedicine.com/NMI/9.4.2.4.htm#p6.

[91] Freitas RA Jr., Nanomedicine, Volume I: Basic Capabilities, Landes Bioscience, Georgetown, TX, 1999, Table 9.5; http://www.nanomedicine.com/NMI/Tables/9.5.jpg.

[92] For high-speed flight, P_{flight} = 38,000 pW at 1 m/sec (http://www.nanomedicine.com/NMI/Tables/9.5.jpg) which could be provided for 10 sec from burst power reserves at an energy cost of 3.8 x 10^5 pJ, or just 16% of the assumed total onboard energy storage of E_{robot} = 2.4 x 10^6 pJ.

[93] Freitas RA Jr., Nanomedicine, Volume I: Basic Capabilities, Landes Bioscience, Georgetown, TX, 1999, Section 9.4.3.5 Legged Ambulation; http://www.nanomedicine.com/NMI/9.4.3.5.htm.

3.3 Facility Mapping

Prior to initiation of the inspection, pre-existing external information that might be available will be collected such as Google maps images, external photographs of the facility, and original floor plans or blueprints on file with local building departments or other government entities.

Early in the on-site inspection mission, comprehensive mapping data regarding the current state of the suspect facility will be collected, These maps will include the current floor plans and the location, geometry and size of all doors, windows, HVAC and fume hood vents, floor drains, and other openings that might allow ready access to the facility from the outside. These maps will also include the location of all electric receptacles and other potential power sources, and the gross surface structure and location of any unmoving objects in each room that could possibly represent a piece of proscribed equipment. The map might be assembled in sequential stages, with a smaller number of inspection robots returning repeatedly to the Delivery Drone outside the facility, uploading their accumulated data to the Drone, then receiving orders from the Drone directing them to the next data collection task to be conducted, or the map could be compiled by a large number of nanorobots operating in parallel to save time. The Delivery Drone will have significant onboard computational capacity and may also have real time communication with large data processing resources possessed by the APM Treaty Compliance Inspection Program authority.

We will now briefly consider a few scaling aspects of this data collection process.

Each wall of an exemplar cubical room of width, height and length L_{room} = 3 meters has a wall surface area of $A_{wall} = L_{room}^2$. Locating features of size $L_{feature} \geq 1$ cm or larger on a wall requires $n_{scan} = L_{room} / L_{feature} = 300$ raster-style traverses of each wall, each traverse of length L_{room}, for a total travel length of $X_{roomscan} = (1 + n_{scan}) L_{room} = 903$ meters. Assuming each wall has one 2x1 meter door (perimeter length 6 meters), ten 10x20 cm electrical outlets each of perimeter length 60 cm (6 meters total), 10 meters of perimeter length for other vents, windows, or other interesting wall features, and an additional 75 meters to provisionally tag the locations of all unmoving objects resting on or attached to each wall, ceiling, or floor (e.g., chairs, tables, equipment racks, overhead cranes, etc.), this gives a total nanorobot linear mapping distance of $X_{wallmap} \sim 1000$ meters, well within the maximum unrecharged $X_{crawl} = 2400$ meter nanorobot crawl range (Section 3.2). At a crawl speed of $v_{crawl} \sim 1$ cm/sec, the entire map path for **one wall** is traversed by a single inspection nanorobot in $t_{wallmap} = X_{wallmap} / v_{crawl} = 100{,}000$ sec (~**1.2 days**).

How might inspection nanorobots track their precise 3D positions in space during their perambulations through the suspect facility? Devices could record their $\hat{x}$, $\hat{y}$, and $\hat{z}$ positional data by keeping careful count of the number of steps they've taken in each direction, given knowledge of step size, a navigational technique known as dead reckoning.[94] However, even small errors in directional or step size measurements may accumulate rapidly, necessitating

---

[94] Freitas RA Jr., Nanomedicine, Volume I: Basic Capabilities, Landes Bioscience, Georgetown, TX, 1999, Section 8.3.1 Dead Reckoning; http://www.nanomedicine.com/NMI/8.3.1.htm.

multiple episodes of re-measure to reduce map errors to acceptable levels, using either multiple passes by the same robots or duplicate simultaneous measurements by multiple robots.

To this end, nanorobots equipped with nanopendular sensors can reliably determine the direction of the local gravity field vector to within ~2 milliradians in ~10^{-4} sec,[95] and gimbaled nanogyroscopes can provide a stable onboard orientation standard, allowing the vertical orientation of the device to be precisely fixed in space – e.g., a generic micron-scale nanogyroscope might suffer a ~1 microradian orientation shift in ~1 hour, ~4 microradians in ~1 day, and ~70 microradians (~10 arcsec) in ~1 year.[96] The positional measurement error across a 3-meter room distance might approximate ~0.6 cm for a 2 milliradian shift and 0.001 cm for a 4 microradian shift. Positional measurement accuracy can be further enhanced by the repeated detection of fixed-position microscale fiducial markers temporarily emplaced at regular intervals on walls, ceilings, and floors.

Inspection nanorobots equipped with even a primitive nanotube radio receiver[97] should also be able to detect external 3D navigational GPS signals retransmitted from a nearby Delivery Drone (Section 3.7)[98] unless the suspect facility is thoroughly shielded. Detection of GPS signals from Drones located ~1 km from the facility may be able to achieve 50-100 cm positional accuracy without advanced correction methods, 1-2 cm positional accuracy using real-time kinematic (RTK) correction,[99] or 0.1-0.2 cm positional accuracy using carrier-phase tracking[100] under optimal conditions.

As a coarse double-check on altitude, nanomechanical gravity sensors can detect variations in local gravity of 10^{-5} g for 11 μm sensors and 10^{-6} g for 20 μm sensors,[101] hence at 45° latitude where g varies from 9.806 m/sec^2 at sea level to 9.803 m/sec^2 at 1000 meters altitude, a 20 μm

---

[95] Freitas RA Jr., Nanomedicine, Volume I: Basic Capabilities, Landes Bioscience, Georgetown, TX, 1999, Section 4.3.4.2 Nanopendulum Orientation Sensing; http://www.nanomedicine.com/NMI/4.3.4.2.htm.

[96] Freitas RA Jr., Nanomedicine, Volume I: Basic Capabilities, Landes Bioscience, Georgetown, TX, 1999, Section 4.3.4.1 Gimballed Nanogyroscopes; http://www.nanomedicine.com/NMI/4.3.4.1.htm.

[97] Jensen K, Weldon J, Garcia H, Zettl A. Nanotube radio. Nano Lett. 2007 Nov;7(11):3508-11; https://ipo.lbl.gov/wp-content/uploads/sites/8/2014/08/2431.pdf.

[98] According to estimates, GPS signals at ~1575 MHz retransmitted from a drone at a power level of ~33 watts using a ~2.5 meter directional dish antenna with a gain of ~1000 should be detected at a distance of ~1 km from the suspect facility by a nanotube radio receiver having the minimum detectable electric field amplitude of 1 V/m/Hz$^{0.5}$ or 60 dBmV/m/Hz$^{0.5}$ reported by Jensen *et al.* (2007).

[99] https://en.wikipedia.org/wiki/Real-time_kinematic_positioning.
[100] https://en.wikipedia.org/wiki/GNSS_enhancement#Carrier-phase_tracking_(surveying).

[101] Freitas RA Jr., Nanomedicine, Volume I: Basic Capabilities, Landes Bioscience, Georgetown, TX, 1999, Section 4.4.2 Nanogravimeters; http://www.nanomedicine.com/NMI/4.4.2.htm.

gravimeter could detect a change in vertical altitude of ~3.3 meters,[102] thus distinguishing among the various floors in a multistory building.

Storing $\hat{x}$, $\hat{y}$, and $\hat{z}$ positional data to within $x_{resolution\text{-}map}$ = 1 cm requires $H_{xyz} \sim 3\ [\log_{10}(L_{room} / x_{resolution\text{-}map})] / \log_{10}(2) \sim 25$ bits per measurement point. Allowing an additional 75 bits for other data of interest gives a total of $H_{datapoint} \sim 100$ bits per measurement point. In each wall scan there are $n_{datapoint} = X_{wallmap} / x_{resolution\text{-}map} = 100{,}000$ measurement points, so the minimum data storage requirement for mapping all ≥ 1 cm features on one wall of the room to 1 mm precision is $H_{wallmap} = n_{datapoint}\ H_{datapoint}$ = **10×10^6 bits**. This data may be stored in mechanical RAM using compact 3D arrays of diamondoid register rods with data density $I_{store} = 10^7$ bits/μm^3 (with ~10^{10} bits/sec access speed),[103] hence the entire data storage requirement for **one complete wall map** can be stored in $V_{RAMwallmap} = H_{wallmap} / I_{store}$ = **1 μm^3 of mechanical RAM** onboard each inspection robot, or only ~0.01% of the total nanorobot volume $V_{robot} = 8000$ μm^3 – or 0.06% of the total volume of one nanorobot to store the mapping data for all 6 walls in a room. Navigation by dead reckoning should be possible for inspection nanorobots traversing hard surfaces with a cumulative positional error of ~0.01%,[104] producing a lateral deviation from straight line of only 0.3 mm at the end of a 3-meter traverse. As previously noted, micron-scale nanopendulum orientation sensors[105] or gimbaled nanogyroscopes[106] will enable the inspection robot to ascertain its orientation relative to gravity at all times, permitting the device to distinguish locomotion in the vertical $\hat{z}$ direction from motion in the horizontal $\hat{x}\hat{y}$ direction and to directly record the travel distance in each direction. Cumulative errors in positional measurements over long distances from the Delivery Drone can be reduced to arbitrarily small values by remapping multiple times at progressively increasing distances from the Delivery Drone, using fixed landmarks (e.g., wall switches, nail holes, etc.) inside the facility as additional checkpoints to re-register and correct inferred positional estimates.

With $n_{roombots}$ = 6 inspection nanorobots assigned to survey the 4 walls, floor, and ceiling of each 3x3 meter ($A_{room} = L_{room}^2 = 9$ m$^2 \sim 97$ ft^2) room, even an enormously large-floor-area $A_{facility}$ = **500,000 ft^2 suspect facility** with $N_{room} = A_{facility} / A_{room} \sim 5200$ room-equivalents could be entirely mapped using a fleet of up to $N_{fleet} = n_{roombots}\ N_{room} \sim$ **31,000 inspection nanorobots** (~0.25 mm^3 total volume) working in parallel over the same $t_{facilitymap} \sim t_{wallmap} \sim$ **1.2 day time**

---

[102] Freitas RA Jr., Nanomedicine, Volume I: Basic Capabilities, Landes Bioscience, Georgetown, TX, 1999, Section 4.9.2.4 Gravitational Geographic Macrosensing; http://www.nanomedicine.com/NMI/4.9.2.4.htm.

[103] Freitas RA Jr., Nanomedicine, Volume I: Basic Capabilities, Landes Bioscience, Georgetown, TX, 1999, Section 10.2.1 Nanomechanical Computers; http://www.nanomedicine.com/NMI/10.2.1.htm.

[104] Freitas RA Jr., Nanomedicine, Volume I: Basic Capabilities, Landes Bioscience, Georgetown, TX, 1999, Section 8.3.1 Dead Reckoning; http://www.nanomedicine.com/NMI/8.3.1.htm.

[105] Freitas RA Jr., Nanomedicine, Volume I: Basic Capabilities, Landes Bioscience, Georgetown, TX, 1999, Section 4.3.4.2 Nanopendulum Orientation Sensing; http://www.nanomedicine.com/NMI/4.3.4.2.htm.

[106] Freitas RA Jr., Nanomedicine, Volume I: Basic Capabilities, Landes Bioscience, Georgetown, TX, 1999, Section 4.3.4.1 Gimballed Nanogyroscopes; http://www.nanomedicine.com/NMI/4.3.4.1.htm.

period. A small 3000 ft^2 suspect facility with N_{room} ~ 31 rooms would require only N_{fleet} ~ 186 inspection robots to compile a comprehensive map in the same amount of time. Various delay factors, including the desire for validation re-mapping, might increase the total facility mapping time to ~1 week, or might increase the total number of required robots if multiple sets of robots are assigned to survey each room for redundancy.

Comparison of the mapped internal structure with the known visible external structure of the suspect facility may reveal the inferable presence of one or more interior rooms of substantial size that have not yet been examined by the first wave of mapping robots. Such rooms might have been missed in the original survey for a variety of reasons ranging from harmless to nefarious. For example, if the missing room is no longer in active use (e.g., an old broom closet), this would explain the absence of human traffic that could have allowed hitchhiking nanorobots to enter and perform their inspection. In this case, the robots probably will have detected a doorway or other conventional access modality. If no door or other means of entry into the missing space is evident, this raises the likelihood of the space possibly being employed for some highly or fully automated purpose, or being deliberately hidden by the operators of the suspect facility – either of which creates additional suspicion. In all cases of hidden rooms, more deliberate robotic means (e.g., Section 3.4) must be employed to explore the unmapped space, including the physical tracing of air ducts, wiring conduits, water or gas pipes, dumbwaiter chutes, foundation seams, and concrete floor slab hairline cracks that are evident in accessible neighboring rooms. If these methods fail, microscopic holes can be drilled through walls (Section 3.5) to allow entry by inspection nanorobots.

Once the facility map has been assembled, all unmoving objects identified within the facility may be ranked by the probability that they might be a piece of proscribed APM equipment. Teams of inspection robots are sent to the most likely candidates for more detailed inspection. The teams slowly work their way through the list of candidate suspect hardware in priority order until some threshold of low probability for the remaining items on the list is reached, allowing the facility inspection to be concluded.

To further enable independent navigation throughout the facility, each robot should carry a simple map of key landmarks to allow it to determine its location (and, for example, the path out of the facility) from any arbitrary location within the facility in which the robot might find itself. Landmarks might include floor-to-ceiling corner lines where two walls come together, door frames, floor drains, lighting fixtures, and the like. Temporary physical markers[107] (ideally invisibly small or well-camouflaged) could be employed to highlight passive landmarks or to serve as active landmarks or navigational trace lines. For instance, one or more separate microscale robots could be assigned to mark and patrol each landmark site to facilitate detection and recognition by traveling nanorobots. A facility with $L_{allwalls} = 8\ N_{room}\ L_{room}$ meters of linear wall space (counting both sides separately) with $n_{landmark} = 1$ landmark per meter and $H_{landmark} = 100$ bits per landmark would require inspection nanorobot onboard memory of $H_{nav} = L_{allwalls}\ n_{landmark}\ H_{landmark} =$ **12.5×10^6 bits** to store **all landmarks** for the huge **500,000 ft^2 facility** mentioned above, taking $N_{room} = 5200$ rooms, $L_{room} = 3$ meters, and $L_{allwalls} = 124{,}800$ meters, or only $H_{nav} = 0.0744 \times 10^6$ bits to store the entire navigational landmark map for the small 3000 ft^2 facility with $N_{room} = 31$ rooms, $L_{room} = 3$ meters, and $L_{allwalls} = 744$ meters.

---

[107] e.g., https://bighorngolfer.com/blogs/a/how-big-can-a-ball-marker-be-in-golf.

3.4 Unconcealed Observables

Once the facility map has been compiled, the full inspection can begin. Unconcealed observables are items of interest that can be observed directly by inspection nanorobots without requiring the robots to destructively penetrate any physical barriers. Upon entering a room to perform their first post-mapping inspection, a nanorobot already possesses the previously-compiled 3D map of all relevant entrances, exits, and power sources in that room. The main objective is to search for evidence of proscribed equipment or activities that exhibit the telltale signs of unregulated APM research, molecular workstations, or nanofactory activity.

Teams of inspection nanorobots will be sent to specific rooms within the suspect facility and tasked to examine specific objects in those rooms.[108] Depending on the nature and duration of the intended search, nanorobots might elect to perform their scans only after they determine: (A) that people are not present inside the room (e.g., by vocalization sensing or chemical scent detection); (B) that the lights are off (or at least the area the robot wishes to inspect is sufficiently dark to evade easy human visual detection); (C) that specific pieces of equipment are or are not in active use (whichever state is relevant to the purpose for which the item is being examined); or (D) the existence of other relevant conditions or restrictions that are necessary to maintain stealth and proper inspection security. Data regarding each of the observables described below may be collected by inspection robots having somewhat different sets of sensors and locomotion systems, but all data should be containable within the exemplar 8000 μm^3 cube-shaped 20-μm inspection nanorobot package previously discussed in Section 3.2.

3.4.1 Principal Unconcealed Observables

During a facility inspection the principal unconcealed observables of interest are:

* **Thermal Observables.** Crawling or airborne nanorobots can take temperature measurements to record the absolute temperature of surfaces, or can collect enough samples to determine thermal spatial or temporal gradients. Cold sources may indicate the presence of operating cryogenic equipment that is venting LN2 or LHe. Heat sources may confirm the presence of operating electric motors, light bulbs, Bunsen burners, or people.

* **Chemical Observables.** Crawling or airborne nanorobots can sample the air to measure and record the concentration of specific chemicals,[109] or spatial[110] or temporal[111]

---

[108] Compliance Program nanorobot mission designers might consider using Regional Managers, e.g., "room manager" control/communication robots, to coordinate activities within each room.

[109] Freitas RA Jr., Nanomedicine, Volume I: Basic Capabilities, Landes Bioscience, Georgetown, TX, 1999, Section 4.2.4 Chemical Assay; http://www.nanomedicine.com/NMI/4.2.4.htm.

[110] Freitas RA Jr., Nanomedicine, Volume I: Basic Capabilities, Landes Bioscience, Georgetown, TX, 1999, Section 4.2.6 Spatial Concentration Gradients; http://www.nanomedicine.com/NMI/4.2.6.htm.

[111] Freitas RA Jr., Nanomedicine, Volume I: Basic Capabilities, Landes Bioscience, Georgetown, TX, 1999, Section 4.2.7 Temporal Concentration Gradients; http://www.nanomedicine.com/NMI/4.2.7.htm.

gradients of chemicals. The presence of a helium or nitrogen gas gradient may confirm the presence of a cryogenic system and indicate its location. Detection of periodic puffs of carbon dioxide in the air may indicate the presence and movement of people. (The movement of specific people around the room might also be tracked via scent detection.) Nanorobots can examine surfaces[112] for their material composition or for the presence of chemical spills, lubricants at seams, and the like. For instance, detection of vacuum grease[113] at a specific surface location on a piece of equipment might help to confirm the presence of a vacuum chamber.

* **Chemical and Biological Samples.** Inspection devices can collect up to picoliter ~$(10\ \mu m)^3$ physical samples of airborne molecules and transport these from the premises to allow detailed analysis elsewhere by APM Treaty Compliance Inspection Program authorities. The detected molecules could range from simple process chemicals to volatilized specialty mechanosynthesis molecular tools, all of which would provide valuable information about the processes being employed in the facility. To maximize the probability of detecting something interesting, collection nanorobots could be positioned on the rims or caps of bottles and vials in the lab, awaiting the opening of the container which would permit direct collection of samples, or near any apparatus that might be used to heat or otherwise volatize process chemicals. Nanorobots could also collect DNA samples or directly read fingerprints from personnel inside the lab to obtain positive confirmation of identity.

* **Atomically Precise Samples.** Inspection devices can crawl around laboratory tables and shelves, inspecting samples for atomically precise structures. Manufactured atomically precise products or their intermediates might be left sitting in the open air in a laboratory or factory facility. Nanorobot engineers must design a general purpose scanning head that can be passed over the surface of any suspect product and conveniently detect the likely presence, or confirm the likely absence, of atomically precise structure. Once a detection has been made, it should be possible to excise a small (1-100 μm^3) sample of the atomically precise structure and store it in an internal compartment, later to transport it out of the suspect facility to allow subsequent more detailed inspection and analysis elsewhere by APM Treaty Compliance Inspection Program authorities.

* **Laboratory Equipment.** Relevant APM laboratory or nanofactory equipment may include UHV vacuum chambers,[114] scanning probe microscopes,[115] displacement metrology systems,[116] cryogenic dewars,[117] vacuum flasks,[118] cryogenic refrigerators,[119] cryogenic

---

[112] Freitas RA Jr., Nanomedicine, Volume I: Basic Capabilities, Landes Bioscience, Georgetown, TX, 1999, Section 4.2.8 Chemotactic Sensor Pads; http://www.nanomedicine.com/NMI/4.2.8.htm.

[113] https://www.thomassci.com/scientific-supplies/Vacuum-Grease.
[114] https://en.wikipedia.org/wiki/Ultra-high_vacuum and https://en.wikipedia.org/wiki/Vacuum_chamber.
[115] https://en.wikipedia.org/wiki/Scanning_probe_microscopy.
[116] https://www.nist.gov/programs-projects/fabry-perot-displacement-interferometry.
[117] https://en.wikipedia.org/wiki/Cryogenic_storage_dewar.
[118] https://en.wikipedia.org/wiki/Vacuum_flask.

[119] Alekseev A. Basics of low-temperature refrigeration, CERN Yellow Report CERN-2014-005, pp.111-139; https://arxiv.org/pdf/1501.07392. Air Liquide offers 80K custom refrigerators for LN2 and LHe from 1-30 KW capacity (https://vtc2017.vtcmag.com/PROD/Products_JUL13/products2.html).

liquefiers,[120] vacuum suitcases,[121] computers, racks of control electronics, coolant supply plumbing, sample preparation systems, and chemical feedstock supply lines. Multiple nanorobots might be tasked to inspect a particular machine or set of interconnected machines. The robots will swarm over the entire external surface of the apparatus, measuring its precise geometry and mapping its accessible wiring and plumbing patterns to 1 mm resolution. If the surface area of an apparatus under inspection ($A_{machine}$) is scanned to a resolution of $x_{resolution\text{-}equip}$ = 1 mm, and if each data point requires $H_{datapoint}$ ~ 100 bits per measurement point (Section 3.3), then the total data requirement for a detailed surface map of a particular apparatus is $H_{apparatus} / A_{machine} = H_{datapoint} / x_{resolution\text{-}equip}^2 = 100 \times 10^6$ bits/m^2 of machine surface that is examined, storable onboard in $V_{RAMequip} = H_{apparatus} / I_{store} = 10$ μm^3 of mechanical RAM of data density $I_{store} = 10^7$ bits/μm^3 which is only ~1.3% of total volume of a single nanorobot, where $H_{apparatus} \sim 10^8$ bits and $A_{machine} \sim 1$ m^2. Shape information alone will often be sufficient to determine the type and function of the machine. The nanorobots can also record to similar spatial resolution the chemical composition (e.g., rubber, aluminum, stainless steel, plastic, etc), surface finish, temperature, and vibration on the exterior surfaces of the machine.

* **Computer Displays**. It should be possible for nanorobots to read and record data displayed on computer or laptop monitors, or on computerized lab notebook displays, located in the room under inspection. Recording everything (emails, passwords, access codes, design drawings, design data, etc.) in real time – which is far more comprehensive than mere keylogging[122] – would require emplacing a thin layer of nanorobot "dust" coating the entire screen,[123] arranged as an array of nanorobots in a predetermined geometric pattern.[124] If readable 11-pt characters appear 3x5 mm in size on the monitor and if a 5x7 dot matrix is sufficient to identify a character, then the task requires ~1 nanorobot per 0.66 mm of linear screen, or ~535,000 robots to completely cover a large 400x600 mm computer monitor, obscuring only 0.09% of the total screen area using invisibly small 20 μm nanorobots. Even for running videos, the data storage requirements should be fairly modest over long periods of data collection because each inspection nanorobot is responsible only for one pixel at a time. For example, at a 60 Hz video refresh rate[125] (~60 bits/sec using a simple 1-bit black/white color scale), **one full week**

---

[120] https://csabg.org/ln2_liquefiers/.

[121] https://www.henniker-scientific.com/products/uhv-sample-transfer-manipulation/vacuum-suitcase, https://www.scientaomicron.direct/28/vacuum-suitcase, or https://www.prevac.eu/en/2,offer/35,vacuum-chambers/20,transport-box-for-vacuum-chamber.html.

[122] https://en.wikipedia.org/wiki/Keystroke_logging.

[123] Normal household, office, and factory dust is in the 1-100 μm size range; https://www.computerdust.com/downloads/special_report_on_the_effect_of_dust_on_electronics.pdf and https://www.oransi.com/page/particle-size.

[124] For example, numbered nanorobots could deploy onto the screen surface in a predetermined pattern, such as a repeating zigzag raster such that the XY position of each device would be specified in advance, with interdevice spacing sufficiently randomized to ensure a distribution similar to room dust.

[125] https://www.trustedreviews.com/news/144hz-monitors-refresh-rate-motion-blur-explained-2948180.

(~600,000 sec) of continuous recording by a robot whose screen position rarely changes requires only **36 x 10^6 bits**, assuming a time stamp is recorded at the start and finish of each continuous data collection period so that the records of all robots can later be synchronized and merged. Nanorobots can also be positioned on keyboards or under individual mechanical keys to provide a direct keylogging function.

* **Written Material.** Nanorobots equipped with appropriate appendages and sensors should be able to read printed or embossed materials by tactile-sensing the slight surface elevations or depressions due to the presence of ink on paper,[126] thread patterns on fabric, or embossing on metal or plastic, or by using a photoelectric sensor to detect reflected light[127] from a weak downward-pointing source that would not be visible to a human naked eye viewing the process from above. Specific observables might include:

(1) Serial numbers, product numbers, performance specifications, and dates stamped on equipment faceplates.

(2) Labels reciting the contents and suppliers of bottles of chemicals or compressed gases.

(3) Shipping labels on boxes containing consumables or equipment that has been ordered and received at the site.

(4) Handwritten laboratory notebooks – nanorobots can scan pages that are open to view, but can also slip between other pages and scan them too. For example, a 15x25 cm notebook page scanned to r_{pixel} = 0.5 mm pixel resolution has N_{pixel} = 150,000 pixels requiring 150,000 bits using a simple 1-bit black/white color scale, and requires $t_{scan} = N_{pixel}\ r_{pixel} / v_{crawl}$ = 7500 sec (~2.1 hours) for a single inspection nanorobot to measure and record, taking v_{crawl} ~ 1 cm/sec. Scanning an entire **200-page notebook**, likely using 200 inspection robots working in parallel, would require only 30 megabits or ~3 μm^3 of 10^7 bit/μm^3 mechanical RAM and would also be completed in ~**2.1 hours**.

(5) Printed books, catalogs, manuals or instruction sheets that are lying on a desk or stacked on shelves, information on whiteboards, and photos or posters affixed to the walls.

(6) Labels or stickers on drawers, doors, windows, or clothing.

(7) URLs, passwords, names, phone numbers, or other information scribbled on Post-It notes, or copied from the computer screen (see above). This information can be handed to cybersecurity experts who can use it to seek out further clues on the objectives and equipment at

---

[126] The typical ink layer on a piece of paper is ~2.5 μm thick on a ~100 μm thick piece of paper. Myllys M, Häkkänen H, Korppi-Tommola J, Backfolk K, Sirviö P, Timonen J. X-ray microtomography and laser ablation in the analysis of ink distribution in coated paper. J Appl Phys. 2015 Apr 14;117:144902; https://jyx.jyu.fi/bitstream/handle/123456789/48554/1/myllysmetal1.4916588.pdf.

[127] This is necessary in cases where the printed ink has been covered with a smooth but clear lamination, which eliminates the topological variations while leaving the text visibly readable.

the suspect facility, possibly by hacking into private websites or accounts and following the trail of evidence to wherever it may lead.

(8) Personal information appearing on documents in employee hip wallets, side purses, or shirt pockets, including driver's licenses, social security cards, passports, credit cards, membership cards, and the like, for the purpose of obtaining positive confirmation of identity.

* **Spoken Conversation**. It will probably be easy to discern the technical objectives being pursued in a laboratory if authorities have access to the casual verbal conversations of engineers or scientists who don't know they're being recorded. Properly configured inspection nanorobots can eavesdrop on conversations held by employees or visitors inside the lab, recording them at high fidelity and reporting them back to the inspection authority. The pressure amplitude of vocalizations in the vicinity of the speaker ranges from $\Delta P_{min} \sim 0.0005$ atm (whispering) to $\Delta P_{min} \sim 0.05$ atm (shouting).[128] The linear size of a cubical nanosensor that can detect these pressures with a Rose-criterion[129] signal/noise ratio of SNR = 5 may be crudely estimated[130] as $L_{sensor} = (k_B T\, e^{SNR} / \Delta P_{min})^{1/3} = 0.05$ μm (shouting) or 0.23 μm (whispering), taking Boltzmann's constant $k_B = 1.38 \times 10^{-23}$ J/K and air temperature T = 300 K. In digital telephony, voice signals are traditionally sampled at 8 KHz using 8-bit bytes or 64,000 bits/sec,[131] so **1 hour of continuous voice recording** requires $H_{voice} = 230 \times 10^6$ bits, storable onboard in $V_{RAMvoice} = H_{voice} / I_{store} = 230\ \mu m^3$ of mechanical RAM which is only ~**2.9% of the volume of one nanorobot**. Thus, even large data streams like audio can be stored by a nanorobot with only a few percent of its internal memory, validating the feasibility of on-board data storage for the mission.

Microscale listening and recording devices can be migrated directly onto headsets or phone speakers, allowing nanorobots to hear and record both sides of telephonic conversations. Such robots could thereby defeat deliberate sound masking[132] of spoken conversations using auditory white noise generators[133] or conventional implementations of the fictional "cone of silence".[134] Listening robots can be emplaced in lab employees' hair, ears, nose, shirts, and so forth,

---

[128] Freitas RA Jr., Nanomedicine, Volume I: Basic Capabilities, Landes Bioscience, Georgetown, TX, 1999, Section 4.9.1.5 Vocalizations; http://www.nanomedicine.com/NMI/4.9.1.5.htm.

[129] "[...] to reduce the number of false alarms to below unity, we will need [...] a signal whose amplitude is 4-5 times larger than the rms noise." Albert Rose, Vision - Human and Electronic, Plenum Press, 1973, p. 10. https://en.wikipedia.org/wiki/Albert_Rose_(physicist) and https://en.wikipedia.org/wiki/Signal-to-noise_ratio#Alternative_definition.

[130] Freitas RA Jr., Nanomedicine, Volume I: Basic Capabilities, Landes Bioscience, Georgetown, TX, 1999, Section 4.5.1 Minimum Detectable Pressure, Eqn. 4.29; http://www.nanomedicine.com/NMI/4.5.1.htm.

[131] https://dsp.stackexchange.com/questions/22107/why-is-telephone-audio-sampled-at-8-khz and https://en.wikipedia.org/wiki/Sampling_(signal_processing)#Sampling_rate.

[132] https://en.wikipedia.org/wiki/Sound_masking.
[133] https://en.wikipedia.org/wiki/White_noise_machine.
[134] https://en.wikipedia.org/wiki/Cone_of_Silence_(Get_Smart).

recording whatever they hear as the person moves from room to room anywhere throughout the suspect facility.

* **Pre-APM SCIFs**. A Sensitive Compartmented Information Facility (SCIF)[135] that has been constructed to conventional specifications[136] without benefit of APM devices, especially if lacking defensive nanorobots or related atomically precise-manufactured instrumentalities, are readily penetrated by inspection nanorobots using methods described elsewhere in this document. Hitchhiking nanorobots inside the SCIF could record spoken conversations, read printed documents, inspect the contents of briefcases, or record data displayed on the monitors of air-gapped computers,[137] then report all this information back to the APM Treaty Compliance Inspection Program authority.

* **Stray Electronic Emissions**. Properly configured inspection nanorobots could detect, measure, and record encoded electromagnetic signals leaking from improperly shielded equipment control lines, computer monitor cables, computer keyboard and USB cables, Ethernet cables, Wi-Fi signals, mobile phone transmissions, and telephone land lines (if any). Such transmissions could be received[138] and recorded, exported to the Delivery Drone outside the facility, then decrypted later with the assistance of the large data processing resources possessed by the APM Treaty Compliance Inspection Program authority. Unstructured emissions from an equipment power cord may confirm that a given apparatus is operating, while providing information on voltage, current, frequency, and power consumption.[139]

* **Missing or Disabled Inspection Nanorobots.** Inspection nanorobots should include a function in which each one reports back through the network, hence to the Drone, that they are still functioning properly, are fully secure and untampered, and have experienced no external interference with their operations. Any pattern of unexplained inspection nanorobot check-in failure or disablement whose benign source cannot be quickly confirmed should trigger prompt withdrawal of all inspection instrumentalities with immediate communication of this event to the Treaty Compliance Inspection authority for quick response by other agencies. Direct discovery of physical evidence (e.g., broken inspection nanorobots) or signal intelligence indicating imminent or actual inspection nanorobot disablement should elicit a similar immediate response.

---

[135] https://en.wikipedia.org/wiki/Sensitive_Compartmented_Information_Facility.

[136] National Counterintelligence and Security Center, "Technical Specifications for Construction and Management of Sensitive Compartmented Information Facilities," Version 1.4, IC Tech Spec – for ICD/ICS 705, 28 Sep 2017; https://www.dni.gov/files/NCSC/documents/Regulations/Technical-Specifications-SCIF-Construction.pdf.

[137] https://en.wikipedia.org/wiki/Air_gap_(networking).

[138] Freitas RA Jr., Nanomedicine, Volume I: Basic Capabilities, Landes Bioscience, Georgetown, TX, 1999, Section 6.4.2 Inductive and Radiofrequency Power Transmission; http://www.nanomedicine.com/NMI/6.4.2.htm and Section 7.2.3 Electromagnetic Broadcast Communication, http://www.nanomedicine.com/NMI/7.2.3.htm.

[139] https://www.powermeterstore.com/category/portable-power-meters, https://www.instrumart.com/MoreAboutCategory?CategoryID=5974.

* **Unidentified Nanorobots**. Inspection nanorobots can sweep walls, floors, desktops, and other freely accessible locations for the presence of foreign nanorobots that are not members of the inspection swarm and are not identifiable as nanorobots legally permitted to be present in the suspect facility. The specific appropriate action to take upon discovering such devices (avoid? inspect? disable? capture?) depends on a multitude of factors but is beyond the scope of the present discussion.

3.4.2 Entry Strategies

It is anticipated that, in most cases, information collected from these unconcealed observables will be sufficient to prove, or at least to form a very strong inference, of the presence or absence of proscribed equipment or activities at the suspect facility.

Treaty violators may anticipate that the authorities will employ inspection nanorobots to investigate their activities, even when the wrongdoers do not themselves yet possess the means to build their own nanorobots that could decisively defeat surveillance by the Treaty Compliance Inspection authority. Such actors may attempt to employ conventional defensive means[140] to frustrate examination by Treaty-sanctioned inspection nanorobots.

For example, all employees entering the suspect facility could be required to strip off all clothing and walk through a personal chemical shower,[141] dunk tank[142] or fumigation chamber,[143] followed by exposure to artificial EMP[144] or UV-C (200-280 nm) ultraviolet irradiation[145] in an attempt to ensure that no nanorobots survive the attempt to hitchhike into the suspect facility.[146] The rinse

---

[140] https://en.wikipedia.org/wiki/Biosafety_level.

[141] Janosko K, Holbrook MR, Adams R, Barr J, Bollinger L, Newton JT, Ntiforo C, Coe L, Wada J, Pusl D, Jahrling PB, Kuhn JH, Lackemeyer MG. Safety Precautions and Operating Procedures in an (A)BSL-4 Laboratory: 1. Biosafety Level 4 Suit Laboratory Suite Entry and Exit Procedures. J Vis Exp. 2016 Oct 3;(116); https://www.ncbi.nlm.nih.gov/pmc/articles/PMC5092084/.

[142] http://labinnovision.com/dunk-tanks/.

[143] Biosafety in Microbiological and Biomedical laboratories, 5th Edition, U.S. Dept. of Public Health, HHS Publication No. (CDC) 21-1112, Dec 2009; https://web.archive.org/web/20160409233223/http://www.cdc.gov/biosafety/publications/bmbl5/BMBL.pdf.

[144] https://en.wikipedia.org/wiki/Electromagnetic_pulse.
[145] https://en.wikipedia.org/wiki/Ultraviolet_germicidal_irradiation.

[146] UV-A (320-400 nm) and UV-B (280-320 nm) are generally not used for antimicrobial sterilization, but these photons can still cause photochemical damage to nanomachinery. Nanorobots equipped with a 250 μm thick aluminum shield have an estimated* mean-time-before-failure of ~10^9 sec at a typical terrestrial daytime irradiance of ~5 W/m^2 (typically ~95% UV-A and ~5% UV-B at ground level). A 10 sec exposure to ~100 W/m^2 UV-A for human skin or eyes, ~20 W/m^2 for skin and ~3 W/m^2 of UV-B for eyes, or 10-20 W/m^2 for skin and 6-10 W/m^2 of UV-C for eyes, are the estimated thresholds for biological damage. Since

water could be sieved to collect dislodged or disrupted nanorobots, thus confirming the attempted intrusion and providing material for examination to help the wrongdoers devise counterstrategies.

To overcome such tactics, Treaty Compliance Inspection authority nanorobots can tightly affix themselves in human hair or can conceal themselves elsewhere on or even inside the human body. A 20 μm nanorobot, smaller in size than the finest grain of sand,[147] will be very difficult to detect by conventional means inside or upon most areas of the body,[148] especially within a wide variety of bodily orifices and crannies, although particles ≥10 μm can be sensed as grit if pressed between the tongue and the roof of the mouth, and particles ≥3 μm retain sensible grittiness when ground between human teeth.[149] Nanorobots hidden on or inside the bodies of suspect facility employees wearing positive pressure isolation suits,[150] chemsuits,[151] or hazmat suits[152] may need to tunnel out of the suit (Section 3.5) or await specific escape opportunities to complete their inspection tasks. Nanorobots can tunnel through HEPA[153] or ULPA[154] filters that might be encountered on air vents without noticeably affecting filter performance, since only small total perforation areas would be required, or can squeeze through microscopic gaps in door seals.

Compliance Program inspection mission designers should also consider periodic data export procedures employing memory-block shuttles in special circumstances requiring large data capture and exfiltration.

---

a nanorobot with a thin aluminum coating could survive many years of normal UV exposure, brief decontamination blasts are not fatal.

[*] Drexler KE. Nanosystems: Molecular Machinery, Manufacturing, and Computation, John Wiley & Sons, New York, 1992, Section 6.5.4, "Photochemical Shielding"; https://www.amazon.com/dp/0471575186/.

[147] A grain of sand may be 50-2000 μm in size; https://hypertextbook.com/facts/2000/IlanaPrice.shtml.

[148] Nanorobots crawling on the skin would likely not be detectable, given the low forces involved and the mean separation of ≥1 mm between adjacent tactile receptors and nociceptors in the human skin; Freitas RA Jr., Nanomedicine, Volume I: Basic Capabilities, Landes Bioscience, Georgetown, TX, 1999, Table 7.3; http://www.nanomedicine.com/NMI/Tables/7.3.jpg.

[149] Freitas RA Jr., Nanomedicine, Volume I: Basic Capabilities, Landes Bioscience, Georgetown, TX, 1999, Section 9.5.1 Dental Walking; http://www.nanomedicine.com/NMI/9.5.1.htm.

[150] https://en.wikipedia.org/wiki/Positive_pressure_personnel_suit.
[151] https://en.wikipedia.org/wiki/NBC_suit.
[152] https://en.wikipedia.org/wiki/Hazmat_suit.
[153] https://en.wikipedia.org/wiki/HEPA.
[154] https://en.wikipedia.org/wiki/Ultra-low_particulate_air.

3.5 Concealed Observables

Concealed observables are items of interest that can be observed by inspection nanorobots only by destructively penetrating physical barriers that may be hiding useful evidence.

After the inspection nanorobots have completed the "unconcealed observables" phase of the inspection mission (Section 3.4), the information they've collected is accumulated and processed by the Delivery Drone parked outside the suspect facility in an unobtrusive location. Subsequent analysis, both locally and in consultation with trained Treaty Compliance personnel and the large data processing resources possessed by the APM Treaty Compliance Inspection Program authorities, may determine that closer scrutiny of certain suspicious equipment will be necessary to finalize a conclusion. In this event, it could become necessary to schedule a third round of physical inspection of the suspect facility that is significantly more intrusive than the first.

By this point in the inspection process, the Treaty Compliance authorities have assembled a comprehensive map of the entire facility, including floor plans, utility connections, security devices, and the location, model number, purpose, and operating status of every possibly significant piece of equipment in the building. The authorities know the power inputs, materials inputs, refrigeration status, and regular working schedules of every important apparatus in every lab and office. Treaty personnel may also have possession of employee lab notebooks, emails, documents and data copied from computer screens, and recorded conversations among key lab personnel or between in-house personnel and absent parties via telephony, possibly over a period of one or more weeks. The authorities should have a very clear idea exactly which pieces of equipment in which rooms remain under suspicion and need to be examined in more intrusive detail.

There are at least two likely scenarios in this situation:

* **Scenario #1**. It is determined that full inspection access to one or more key rooms, or to one or more key pieces of equipment, has somehow been denied, or there appears to be evidence of corruption or tampering with the inspection data collected by the nanorobots, or with the nanorobots themselves. This calls into question the working assumption that the suspect facility is protected only by conventional means, and not by more effective nanorobotic means (e.g., local defensive patrol nanorobots) – a conclusion that would remove further responsibility for dealing with the situation from the APM Treaty Compliance Monitoring Program, since Program assets are unable to provide further useful information that might resolve the matter. Other means would then need to be employed to deal with this likely Treaty violation.

* **Scenario #2**. The "unconcealed observables" phase of the inspection mission (Section 3.4) has uncovered evidence that one or more rooms might harbor illegal equipment or activities, but the existing data are insufficient to definitively confirm or rule out this possibility. Additional direct physical evidence is required in this case.

In Scenario #2, the first task is to prepare a short list of all still-suspect equipment that needs to be revisited more intrusively, and then to dispatch the appropriate inspection robots to perform a more aggressive "concealed observables" inspection on the suspect equipment. Perhaps the most likely piece of such suspect equipment will be some form of cryogenic chamber, partially or wholly under UHV, in which an SPM workstation or nanofactory is being operated to fabricate intermediate ramp-related APM nanomachinery or finished APM products. Intermediate or finished APM products may be contained somewhere inside the vacuum chamber or might reside

in a vacuum suitcase, locked container, vial, or wall safe somewhere on the premises. A means of access to the interiors of these containers therefore must be defined.

The simplest procedure is to employ a second species of inspection nanorobots that can perform drilling operations. The drilling robots will tunnel through container walls, creating a channel through which the somewhat smaller inspection robots can travel, enabling detection, measurement, characterization, and then imaging or sampling of whatever lies hidden within. Scaling laws favor the largest possible drilling robot, since the volume of material to be excavated to a fixed depth increases as the cross-sectional area of the robot and its hole ($\sim L_{robot}^2$), while the available drilling energy increases as the volume of the robot ($\sim L_{robot}^3$) if energy storage represents a fixed fraction of robot volume.

Consider an exemplar large cube-shaped drilling nanorobot of size L_{robot} = **100 µm** and volume $V_{robot} = L_{robot}^3$ = 1,000,000 µm^3, with $f_{storage}$ = 10% of robot volume allocated to some optimal combination of battery (continuous) and mechanical (burst) energy storage, or $V_{storage} = f_{storage} V_{robot}$ = 100,000 µm^3, giving the robot $E_{robot} = E_D V_{storage}$ = **3 x 10^8 pJ** of combined battery and burst energy to draw upon, conservatively taking $E_D \sim 3$ MJ/L.[155] A ~100 µm^3 **electrical energy tap primary recharge system** generating $P_{tap} \sim 1 \times 10^{-5}$ W of recharge power (Section 3.2) permits the entire onboard energy store to be recharged in $t_{recharge,tap} \sim E_{robot} / P_{tap}$ = **30 sec**. The photovoltaic system can provide continuous recharge power by coating at least all of one cube face with photovoltaic cells, covering $A_{voltaic} = L_{robot}^2$ = 10,000 µm^2 of robot surface and occupying an additional $V_{voltaic} = (I_{photo} / P_{D,photo}) A_{voltaic}$ = 5000 µm^3, or $f_{voltaic} = V_{voltaic} / V_{robot}$ = 0.5% of robot volume, producing up to $P_{voltaic} = I_{photo} A_{voltaic}$ = 20,000 pW of continuous power under typical indoor illumination which is enough to **photovoltaically recharge** the entire onboard energy store in $t_{recharge,photo} \sim E_{robot} / P_{voltaic}$ = 15,000 sec (~**4.2 hours**), taking $I_{photo} \sim 2$ pW/µm^2 and photovoltaic power density $P_D \sim 4$ pW/µm^3 (Section 3.2).

The drilling robot burrows a **microscopic hole** of area $A_{hole} \sim L_{robot}^2$ = **10,000 µm^2** and depth d_{hole} = **5 mm** (≈ typical thickness[156] for a cold-rolled stainless steel vacuum chamber wall). Iron, the main component of stainless steel,[157] has 0.055845 kg/mole and a density near room temperature of 7874 kg/m^3,[158] hence a molar volume of $V_{molarFe}$ = 8.49 x 10^{10} Fe atoms/µm^3. The bond energy of Fe atoms in metallic solids is E_{Fe} = 418 kJ/mole = 6.94 x 10^{-19} J/atom,[159] hence drilling the

---

[155] Freitas RA Jr. Energy Density. IMM Report No. 50, 25 June 2019, Table 24. Specific energy, energy density, specific power and power density for batteries and fuel cells; http://www.imm.org/Reports/rep050.pdf.

[156] e.g., David Garton, Vacuum Technology and Vacuum Design Handbook for Accelerator Technicians, Appendix 1 – Structural Calculations for Scientific Vacuum Vessel Design. ANSTO/E-775, Nov 2011; http://apo.ansto.gov.au/dspace/bitstream/10238/4126/1/Vacuum%20Technology%20and%20Vacuum%20Design%20Handbook%20for%20Accelerator%20Technicians%20%282%29.pdf.

[157] http://www.ssina.com/composition/chemical.html.
[158] https://en.wikipedia.org/wiki/Iron.

[159] Freitas RA Jr. Energy Density. IMM Report No. 50, 25 June 2019, Table 43. Specific energy of solid metal formation from neutral metal atoms; http://www.imm.org/Reports/rep050.pdf.

proposed hole may cost as much as $E_{hole} \sim d_{hole} A_{hole} V_{molarFe} E_{Fe} = 2.95 \times 10^{12}$ pJ.[160] This will require a fleet of $N_{robot} \sim E_{hole} / E_{robot} \sim$ **10,000 drilling robots**, with each robot excavating only 1/10,000th of the hole until its onboard energy is exhausted, then promptly vacating the site to make room for the next fully charged drilling robot to immediately take its place and resume drilling. If each robot drills at a P_{drill} = 10,000,000 pW power level (robot power density $P_{D,robot} = P_{drill} / V_{robot} \sim 10^7$ W/m^3),[161] then the hole is completed in $t_{drill} \sim (E_{robot} / P_{drill}) N_{robot} \sim 3 \times 10^5$ sec (~**3.5 days**) by the fleet of 10,000 robots. Alternatively, the same mission can be completed by a nanorobot fleet that delivers 10,000 total drilling robot visits, using a lesser number of robots that are periodically recharged locally and then return to the task.

A 100 μm diameter drilling nanorobot will likely be visible to the naked eye in normal lighting,[162] especially if it is moving against a high-contrast background. Therefore these larger robots should only move during cover of darkness or in poor lighting, and their drill hole sites should be chosen so as to be minimally visible to human operators who may be periodically visually inspecting the apparatus.[163] Judicious choice of the drilling site can minimize the total number of holes to be drilled. For example, by carefully selecting the pressure relief value on the central tube of the vacuum system for the drilling site (image, left), the robot may only need to create a single hole to give the smaller inspection nanorobots complete access to the interior sample stage. Once inside, those inspection robots can physically examine the SPM probe tip that may be directly manipulating (1) surface-bound tooltip molecules, (2) workpieces and intermediate structures on the surface or the probe apex, or (3) finished atomically precise structures or devices clustered on the surface of the sample.

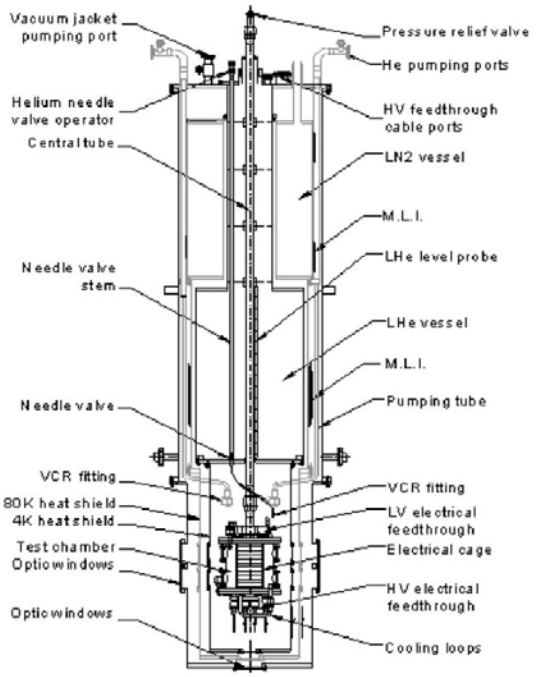

A nanorobot burrowing into a hollow chamber under full vacuum would have to very quickly emplace a cover plate over the atmosphere-facing side of the hole to prevent air from rapidly

---

[160] This should be an upper limit because material may be drilled out in such a way as to minimize the number of bond breakages, e.g., by removing material in chunks.

[161] Freitas RA Jr., Nanomedicine, Volume I: Basic Capabilities, Landes Bioscience, Georgetown, TX, 1999, Section 9.3.5.3.5 Molecular Mechanodecomposition; http://www.nanomedicine.com/NMI/9.3.5.3.5.htm.

[162] A grain of sand may be 50-2000 μm in size; https://hypertextbook.com/facts/2000/IlanaPrice.shtml.

[163] Energy scaling alone might favor a cylindrical robot shape over a spherical or cubic shape, as this would minimize the volume of material to be excavated, but such a robot would have at least one dimension much longer than 100 μm which might enhance visibility and increase the risk of detection by human eyes.

flowing through the hole and into the vacuum, creating a pressure rise (see below) that would be detectable almost immediately by experimentalists operating the equipment.[164] Creating a workable cover plate is not a problem. Consider again our exemplar cube-shaped drilling nanorobot with edge length L_{robot} that has drilled a square microhole of cross-sectional area $A_{robot} = L_{robot}^2$ through a vacuum chamber wall, creating a pressure differential of ΔP_{hole} between the interior vacuum and the external laboratory air. The robot can prevent the entry of air through the microhole by temporarily emplacing over the microhole a square cover plate of edge length edge L_{plate}, area $A_{plate} = L_{plate}^2$, thickness h_{plate}, and Young's modulus E_{plate} which, when clamped on all four sides and loaded by a uniform pressure differential of ΔP_{hole}, will exhibit a maximum out-of-plane deflection at the center of the plate of $\delta_{plate} = k_{plate} (\Delta P_{hole} L_{plate}^4 / E_{plate} h_{plate}^3)$, where k_{plate} is a constant of order ~0.1.[165] Taking $E_{plate} = 1.05 \times 10^{12}$ N/m^2 for diamond, $\Delta P_{hole} = 1$ atm, $L_{plate} = L_{robot} = 100$ μm, a $\delta_{plate} = 0.01 L_{plate} = 1$ μm (~1% center deflection) requires a cover plate of thickness $h_{plate} = [k_{plate} (\Delta P_{hole} L_{plate}^4 / \delta_{plate} E_{plate})]^{1/3} = 1$ μm and volume $V_{plate} = h_{plate} L_{plate}^2 = 10{,}000$ μm^3. With proper design, a cover plate of this volume could be carried inside ~1% of the volume of one 1,000,000 μm^3 drilling robot and later unfolded for use at the microhole site.

However, the leak rate through a microscopic hole with a ~1 atm pressure differential can quickly ruin an ultra-high vacuum (UHV) internal environment. This rate is readily estimated from the Hagen-Poiseuille Law which states that a pressure differential of ΔP between the ends of a cylindrical pinhole leak channel of radius $r_{pinhole}$ and length $L_{pinhole}$ will move an incompressible fluid of absolute viscosity η in laminar flow at a volume rate of $Q = \pi r_{pinhole}^4 \Delta P / 8 \eta L_{pinhole}$.[166] Over an observation period of duration t_{leak} the pressure inside a chamber of volume $V_{chamber}$ will initially increase by $\Delta P_{chamber} \sim \Delta P (Q t_{leak} / V_{chamber}) = (2.61 \times 10^{-5}) t_{leak}$ atm, taking $\eta = 1.9 \times 10^{-5}$ kg/m-sec for 300 K air at 1 atm pressure,[167] $r_{pinhole} \sim 50$ μm for a drilling nanorobot, $L_{pinhole} = 5$ mm for the stainless steel wall of a vacuum chamber of volume $V_{chamber} = 0.1$ m^3, and $\Delta P = 1$ atm for a vacuum chamber located in a lab with normal air, with air flowing through the pinhole into the chamber at $Q = 2.61 \times 10^{-6}$ m^3/sec.

---

[164] Such hermetic cover plates may not be needed by robots penetrating a door, wall safe, glass bottle container, or similar interface where there is no significant air/liquid pressure/composition difference on either side of the barrier.

[165] Stephen P. Timoshenko, Theory of Plates and Shells, McGraw-Hill/United Engineering Trustees, New York, 1940; Ansel C. Ugural, Stresses in Plates and Shells, Second Edition, McGraw-Hill Higher Education, New York, 1998. Samuel Levy, Samuel Greenman, "Bending with large deflection of a clamped rectangular plate with length-width ratio of 1.5 under normal pressure," National Advisory Committee for Aeronautics (NACA), Washington DC, Technical Note 853, 1942; http://naca.larc.nasa.gov/reports/1942/naca-tn-853/. Prof. Dr.-Ing. Kai-Uwe Bletzinger, "Theory of Plates, Part II: Plates in bending," Lehrstuhl fur Statik, Technische Universitat Munchen, Lecture Notes, Winter Semester 2000/2001; http://www.statik.bauwesen.tu-muenchen.de/vorlesungen/plates.dir/plates_part2.pdf.

[166] Freitas RA Jr., Nanomedicine, Volume I: Basic Capabilities, Landes Bioscience, Georgetown, TX, 1999, Section 9.2.5 Pipe Flow; http://www.nanomedicine.com/NMI/9.2.5.htm.

[167] Freitas RA Jr., Nanomedicine, Volume I: Basic Capabilities, Landes Bioscience, Georgetown, TX, 1999, Table 9.4; http://www.nanomedicine.com/NMI/Tables/9.4.jpg.

If a UHV molecular workstation or nanofactory typically operates at $P_{WS} \sim 10^{-15}$ atm (~10^{-12} torr), then pinhole exposure times on the order of $t_{leak1} \sim P_{WS} / (2.61 \times 10^{-5}$ atm/sec) = 4×10^{-11} sec doubles the internal pressure, and the declining vacuum leaves the UHV range altogether in $t_{leak2} \sim (10^{-12}$ atm) / (2.61×10^{-5} atm/sec) = 4×10^{-8} sec. Even reducing the diameter of the burrowing nanorobot by tenfold to $r_{pinhole}$ = **5 μm** would only increase these **leak times** to $t_{leak1} \sim P_{WS} / (2.61 \times 10^{-9}$ atm/sec) = 4×10^{-7} sec and $t_{leak2} \sim (10^{-12}$ atm) / (2.61×10^{-9} atm/sec) = **4×10^{-4} sec**, with Q = 2.61×10^{-10} m^3/sec.[168] This suggests that: (A) burrowing nanorobots should only drill their holes when the vacuum chamber is not yet evacuated, or (B) after making the ~100 μm hole these robots should install inside the hole a high-quality airlock[169] mechanism that will allow the smaller (~20 μm) inspection robots to readily pass through the hole, entering or exiting the chamber without breaking the UHV vacuum. A properly designed "manhole cover" hiding an airlock portal ~20 μm in size should not be readily visible upon inspection by the human eye.

Dangerous Discovery. If inspection robots encounter anything resembling a diamond-encased "sealed assembler laboratory"[170] or equivalent entity, all efforts to penetrate its outer surfaces

---

[168] If the UHV chamber is operated at cryogenic temperatures, intruding oxygen or nitrogen gas from inrushing air should quickly freeze out on the cold interior chamber walls, forestalling some or all of the otherwise observable pressure rise. However, contamination of the internal environment is still likely and would also be observable by the equipment operator, though perhaps with some time delay.

[169] https://en.wikipedia.org/wiki/Airlock.

[170] Drexler KE. Engines of Creation, Doubleday, 1986, pp. 184-5; https://web.archive.org/web/20030212122242/https://foresight.org/EOC/EOC_Chapter_11.html#section04of05: "Picture a computer accessory the size of your thumb, with a state-of-the-art plug on its bottom. Its surface looks like boring gray plastic, imprinted with a serial number, yet this sealed assembler lab is an assembler-built object that contains many things....The end of this thumb-sized object holds a sphere built in many concentric layers. Fine wires carry power and signals through the layers; these let the nanocomputer in the base communicate with the devices at the sphere's center. The outermost layer consists of sensors. Any attempt to remove or puncture it triggers a signal to a layer near the core. The next layer in is a thick spherical shell of prestressed diamond composite, with its outer layers stretched and its inner layers compressed. This surrounds a layer of thermal insulator which in turn surrounds a peppercorn-sized spherical shell made up of microscopic, carefully arranged blocks of metal and oxidizer. These are laced with electrical igniters. The outer sensor layer, if punctured, triggers these igniters. The metal-and-oxidizer demolition charge then burns in a fraction of a second, producing a gas of metal oxides denser than water and almost as hot as the surface of the Sun. But the blaze is tiny; it swiftly cools, and the diamond sphere confines its great pressure. This demolition charge surrounds a smaller composite shell, which surrounds another layer of sensors, which can also trigger the demolition charge. These sensors surround the cavity which contains the actual sealed assembler lab…. These elaborate precautions justify the term "sealed." Someone outside cannot open the lab space without destroying the contents, and no assemblers or assembler-built structures can escape from within. The system is designed to let out information, but not dangerous replicators or dangerous tools. Each sensor layer consists of many redundant layers of sensors, each intended to detect any possible penetration, and each making up for possible flaws in the others. Penetration, by triggering the demolition charge, raises the lab to a temperature beyond the melting point of all possible substances and makes the survival of a dangerous device impossible. These protective mechanisms all gang up on something about a millionth their size – that is, on whatever will fit in the lab, which provides a spherical work space no wider than a human hair....Though small by ordinary standards, this work space holds room enough for millions of assemblers and thousands of trillions of atoms. These sealed labs will let people build and test devices, even voracious replicators, in complete safety."

should be halted at once. The device should be externally mapped, its location and time of discovery recorded, and this information should be communicated to the Treaty Compliance Inspection authority with all possible haste. Such a diamond-walled object may enclose highly dangerous nanodevices and, if unregistered with the APM Treaty Compliance Inspection Program authority, almost certainly represents a Treaty violation of the highest order.

3.6 Self-Destruct Protocol

The APM Treaty Compliance Inspection Program authority may prefer that its inspection instrumentalities not fall into the hands of suspected Treaty violators, who might be able to examine and reverse-engineer them, or devise potent countermeasures. Thus, as an additional security measure, inspection nanorobots may need to be equipped with a self-destruct mechanism in case they break down, become trapped, or their presence or activities in a suspect facility are recognized. The self-destruct protocol should be engaged if the robot determines that: (A) its presence has been detected, (B) something is trying to capture or examine it, (C) it is malfunctioning seriously enough to prevent return to the Drone, or (D) some other indicator of serious mission failure has occurred.

The first part of the self-destruct procedure should be to erase all data caches that have been collected during the surveillance activities. The next step should be to erase all software and security keys that are not essential to the process of self-destruction. The robot should then attempt to quickly (~1 sec) relocate to a position of minimum visibility nearby, and then, if possible, self-immolate.

A robot made mostly of diamond should burn in oxygen quite nicely if sufficient oxygen is readily available. Consider an inspection nanorobot of volume V_{robot} composed of a fraction $f_{diamond}$ by volume of solid diamond with carbon atom number density $n_{carbon} \sim 176$ C atoms/nm^3. The least oxygen-demanding combustion pathway would combine one carbon atom with one oxygen atom to make one molecule of carbon monoxide (e.g., $C + \frac{1}{2}O_2 \rightarrow CO$), which occurs when carbon is burned in a limited supply of oxygen or air.[171] (The production of CO is thermodynamically favored over CO_2 at temperatures above ~700 °C,[172] and thus also at the 700-900 °C combustion temperature of diamond in air.[173]) The minimum number of oxygen molecules required to consume all carbon atoms in an inspection nanorobot would therefore be $N_{O2} = n_{carbon}\, f_{diamond}\, V_{robot} / 2$. If the number density of O_2 molecules compressed to 10,000 atm in an onboard diamond pressure vessel is $n_{O2} = 177 \times 10^{26}$ O_2 molecules/m^3,[174] then the volume of compressed oxygen needed to completely burn an inspection nanorobot to carbon monoxide gas is $V_{O2} = N_{O2} / n_{O2} = n_{carbon}\, f_{diamond}\, V_{robot} / 2\, n_{O2} \sim 20{,}000$ μm^3, taking $V_{robot} = 8000$ μm^3 for total robot volume and $f_{diamond} = 0.5$. Therefore it appears that complete nanorobot immolation using only onboard compressed O_2 as the oxidant is not feasible.

---

[171] https://en.wikipedia.org/wiki/Carbon_monoxide#Industrial_production.
[172] https://en.wikipedia.org/wiki/Ellingham_diagram.

[173] F. Albert Cotton, Geoffrey Wilkinson, Advanced Inorganic Chemistry: A Comprehensive Text, Second Edition, John Wiley & Sons, New York, 1966, p. 296. Max Bauer, Precious Stones, Volume 1. Dover Publications, 2012, pp. 115-117. See also: https://www.gemsociety.org/article/can-diamonds-burn/, https://www.gia.edu/diamond-care-cleaning, and https://web.archive.org/web/20170628094809/http://sciencequestionswithsurprisinganswers.org/2014/03/27/can-you-light-diamond-on-fire/.

[174] Freitas RA Jr., Nanomedicine, Volume I: Basic Capabilities, Landes Bioscience, Georgetown, TX, 1999, Table 10.2; http://www.nanomedicine.com/NMI/Tables/10.2.jpg.

However, inspection nanorobots located in a normal atmospheric environment with ~21% O_2 content can draw oxygen from the air to help carry the combustion process to completion. An onboard pressure tank containing 10,000-atm compressed O_2 representing ~5% of robot volume (~400 μm^3 of O_2) could combustively consume ~2% (~160 μm^3) of whole-robot volume. Internal combustion pathways can be designed to maximize heat generation and to include multiple channels leading to the external environment to give atmospheric oxygen ready access to the conflagration, allowing the entire robot to be quickly consumed once the burn has been initiated.[175] If external sensors determine that the robot is surrounded by an oxygen-free environment (e.g., the robot has been relocated to liquid nitrogen or water, or the surrounding air is pure N_2, Ar, or CO_2, or if the robot is in a vacuum), then the combustion pathways should be designed to preferentially destroy the most sensitive or technologically-revealing atomically precise structures inside the robot.

The possibility of merging two devices to enable a more complete self-destruct capability when crucial in special locations (e.g., inside UHV) should be investigated as another design alternative.

[175] Diamond powder of small grain size (~50 μm) burns with a shower of red-orange sparks after ignition from a flame. Lederle F, Koch J, Hübner EG. Colored Sparks. Euro J Inorg Chem. 2019 Feb 21; 2019(7):928–937; https://onlinelibrary.wiley.com/doi/abs/10.1002/ejic.201801300.

3.7 Delivery Drone

The Delivery Drone must coordinate at least semi-automated collection of data on the architecture (e.g., surface mapping) and both unconcealed and concealed observables in the suspect facility to which the Drone has been assigned. The Delivery Drone might resemble a small bird, or a piece of equipment camouflaged to avoid drawing attention.

To conduct floor, ceiling, and wall surface mapping of a huge 500,000 ft^2 suspect facility (the most demanding scenario due to size), surface maps for a 5200-room facility require a minimum of $N_{wallbot}$ = 31,000 nanorobots (Section 3.3), each at most $L_{wallbot}$ = 20 μm in size requiring a minimum robot volume of $V_{wallbot} \sim N_{wallbot} L_{wallbot}^3$ = 0.25 mm^3 of wallbots. Each wallbot stores one $H_{wallmap} = 10 \times 10^6$ bit wallmap and one $H_{nav} = 12.5 \times 10^6$ bit landmark map (Section 3.3), so the total data storage for all facility walls and landmarks is $H_{walls} = N_{wallbot} (H_{wallmap} + H_{nav}) = 7 \times 10^{11}$ bits. The data storage volume requirement onboard the Drone for facility mapping is $V_{RAMwalls} = H_{walls} / I_{store} \sim 70{,}000$ μm^3 of mechanical RAM, taking $I_{store} = 10^7$ bits/μm^3 (Section 3.3). This minimal wall inspection nanorobot fleet could easily be increased 100- or 1000-fold, whether for redundancy or to ensure completeness and survey rapidity, without materially affecting the total requirements for surveying unconcealed observables (see below).

To survey all unconcealed observables in a 500,000 ft^2 suspect facility (Section 3.4), the four most data- and nanorobot-intensive data collection requirements are of four kinds:

(1) **Laboratory Equipment.** Assuming each of the N_{room} = 5200 rooms in the facility has $n_{equipment}$ = 1000 pieces of equipment needing mapping and each piece of equipment has $A_{machine} \sim 1$ m^2 of mappable surfaces with $H_{apparatus} / A_{machine} \sim 100 \times 10^6$ bits/m^2 (Section 3.4.1), then the data requirement for scanning all lab equipment in the facility is $H_{facilityLE} = N_{room}$ $n_{equipment}$ $A_{machine}$ $(H_{apparatus} / A_{machine}) = 5.2 \times 10^{14}$ bits, requiring $V_{RAM\text{-}LE} = H_{facilityLE} / I_{store} = 5.2 \times 10^7$ μm^3 (0.052 mm^3) of Drone onboard mechanical RAM and $N_{LEbot} \sim V_{RAM\text{-}LE} / V_{RAMequip}$ = 520,000 inspection nanorobots ($V_{RAMequip} \sim 100$ μm^3; Section 3.4.1) of total volume $V_{LEbot} = N_{LEbot} L_{wallbot}^3$ = **4.2 mm^3** of Laboratory Equipment inspection nanorobots to be carried onboard the Drone.

(2) **Computer Displays.** Assuming each of the N_{room} = 5200 rooms in the facility has $n_{screens}$ = 10 computer screens to be continuously monitored using $N_{screenbot}$ = 535,000 nanorobots per screen with each robot recording $H_{screenbot} = 36 \times 10^6$ bits/robot during one week of uninterrupted surveillance, then the data requirement for scanning all display equipment in the facility is $H_{facilityCD} = N_{room}$ $n_{screens}$ $N_{screenbot}$ $H_{screenbot} = 1.0 \times 10^{18}$ bits, requiring $V_{RAM\text{-}CD} = H_{facilityCD} / I_{store}$ = 100 mm^3 of Drone onboard mechanical RAM and $N_{CDbot} = N_{room}$ $n_{screens}$ $N_{screenbot} = 2.78 \times 10^{10}$ inspection nanorobots of total volume $V_{CDbot} = N_{CDbot} L_{wallbot}^3$ = **223 cm^3** of Computer Display inspection nanorobots to be carried onboard the Drone.

(3) **Written Material.** Assuming each of the N_{room} = 5200 rooms in the facility has $n_{notebook}$ = 100 handwritten laboratory notebooks to be copied with n_{page} = 200 pages per notebook and H_{page} = 150,000 bits/page, then the data requirement for scanning all notebooks in the facility is $H_{facilityWM} = N_{room}$ $n_{notebook}$ n_{page} $H_{page} = 1.56 \times 10^{13}$ bits, requiring $V_{RAM\text{-}WM} = H_{facilityWM} / I_{store} = 1.6 \times 10^6$ μm^3 of Drone onboard mechanical RAM and $N_{WMbot} \sim N_{room}$ $n_{notebook}$ $n_{page} = 104 \times 10^6$ inspection nanorobots of total volume $V_{WMbot} = N_{WMbot} L_{wallbot}^3$ = **0.83 cm^3** of Written Material inspection nanorobots to be carried onboard the Drone.

(4) **Spoken Conversations.** Assuming each of the N_{room} = 5200 rooms in the facility has $n_{talkers}$ = 10 human talkers to be recorded, generating $H_{voice} = 230 \times 10^6$ bits/hour of continuous

speech for a t_{talk} = 24 hour surveillance period, then the data requirement for recording all talkers in the facility is $H_{facilitySC} = N_{room}\ n_{talkers}\ H_{voice}\ t_{talk}$ = 2.87 x 10^{14} bits, requiring $V_{RAM\text{-}SC} = H_{facilitySC} / I_{store}$ = 2.9 x 10^{7} μm^3 of Drone onboard mechanical RAM and $N_{SCbot} \sim H_{facilitySC} / H_{voice}$ = 1.25 x 10^{6} inspection nanorobots (assuming each robot records an average of one hour of continuous talking) of total volume $V_{SCbot} = N_{SCbot}\ L_{wallbot}^{\ 3}$ = **10 mm^3** of Spoken Conversation inspection nanorobots to be carried onboard the Drone.

To capture other unconcealed observables and to allow for redundant operation with plenty of spares during the inspection of a huge 500,000 ft^2 suspect facility, we shall assume that the Drone must transport and manage ~5 times the number of robots and bits tallied above. Hence the Delivery Drone must carry $N_{Dronebots} = 5\ (N_{LEbot} + N_{CDbot} + N_{WMbot} + N_{SCbot}) \sim 0.14$ x 10^{12} inspection nanorobots of volume $V_{Dronebots} = N_{Dronebots}\ L_{wallbot}^{\ 3} \sim 1100$ cm^3 (~**1 liter**) and must be able to store at least $H_{Drone} = 5\ (H_{facilityLE} + H_{facilityCD} + H_{facilityWM} + H_{facilitySC}) \sim 5$ x 10^{18} bits of inspection data requiring $V_{RAM\text{-}Drone} = H_{Drone} / I_{store} \sim 0.5$ cm^3 of Drone onboard mechanical RAM. Smaller suspect facilities will have correspondingly smaller Delivery Drone nanorobot transport and data storage requirements.

Drone requirements for concealed observables (Section 3.5) will vary widely according to the type of facility and the activities sought to be concealed. It seems unlikely that the nanorobot volume and data requirement will exceed those already estimated above for the unconcealed observables. For example, the use of 10,000 drilling nanorobots each of size L_{robot} = 100 μm and volume $L_{robot}^{\ 3}$ = 1,000,000 μm^3 have a fleet volume of ~0.01 cm^3, so that 100 drilling missions would require the Drone to transport only an additional ~1 cm^3 of devices.

The computational power required by the Drone must be low enough so that its energy (heat) signature is not easily detectable. Assuming that the entire data cache of H_{Drone} = 5 x 10^{18} bits must be processed at least once in a t_{Drone} ~24 hour cycle time, and assuming that processing each bit of this data requires $K_{Drone} \sim 1000$ bits/bit of computational effort, then the continuous onboard data processing rate is $i_{Drone} \sim K_{Drone}\ H_{Drone} / t_{Drone}$ = 5.8 x 10^{16} bits/sec. According to classical descriptions of high-density nanocomputing,[176] a 3D diamondoid logic-rod CPU can achieve a specific processing power of $U_{nano} \sim 10^{30}$ bit/sec-m^3,[177] which implies the Drone will need a nanocomputer CPU of approximate volume $i_{Drone} / U_{nano} \sim 58{,}000$ μm^3. A mechanical computing system[178] that could make full use of reversible computing and built using the kind of

---

[176] Drexler KE. Nanosystems: Molecular Machinery, Manufacturing, and Computation, John Wiley & Sons, New York, 1992, Chapter 12 "Nanomechanical Computational Systems"; https://www.amazon.com/dp/0471575186/. Freitas RA Jr., Nanomedicine, Volume I: Basic Capabilities, Landes Bioscience, Georgetown TX, 1999, Section 10.2.1, "Nanomechanical Computers"; http://www.nanomedicine.com/NMI/10.2.1.htm.

[177] Assuming 1 GHz operation of a (400 nm)^3 CPU,[*] and using 64-bit words: (64 bits/operation) (10^9 operations/sec) / (400 nm)^3 = 1 x 10^{30} bits/sec-m^3.

[*] Drexler KE. Nanosystems: Molecular Machinery, Manufacturing, and Computation, John Wiley & Sons, New York, 1992, Chapter 12 "Nanomechanical Computational Systems"; https://www.amazon.com/dp/0471575186/.

[178] Merkle RC, Freitas RA Jr., Hogg T, Moore TE, Moses MS, Ryley J. Mechanical computing systems using only links and rotary joints. J Mechanisms Robotics 2018 Dec;10(6):061006; https://arxiv.org/pdf/1801.03534.pdf.

mature nanotechnology that will be available in the Treaty Compliance era should be able to achieve ~10^{12} GFLOPS/watt or ~10^{-21} J/bit assuming erasure of one bit for every logical operation.[179] This is very close to the experimentally-confirmed[180] classical Landauer limit[181] for non-reversible computational energy dissipation of $E_{Landauer300K} \sim k_B T \ln(2)$ J/bit = 2.9 x 10^{-21} J/bit using a room temperature nanocomputer at T = 300 K, taking Boltzmann's constant k_B = 1.38 x 10^{-23} J/K. This implies a continuous power draw of $P_{Drone} \sim i_{Drone}\ E_{Landauer300K} \sim 0.17$ mW for these computations, producing a minuscule blackbody emission temperature increase of $\Delta T = T_{Drone} - T_{ambient} = [T_{ambient}^4 + (P_{Drone} / e\ \sigma\ A_{Drone})]^{1/4} - T_{ambient} \sim$ **28 microkelvins**, taking $T_{ambient}$ = 300 K, drone emission surface area $A_{Drone} \sim 1\ m^2$, emissivity e ~ 1, and σ = 5.67 x 10^{-8} W/m^2-K^4 (Stefan-Boltzmann constant).

Wild animals such as rodents will have much larger infrared signatures than the Drone. For instance, a single wild rat with a basal metabolism of ~1 watt and a ~100 cm^2 cross-sectional area emits ~100 W/m^2, which is 50,000-fold higher than the ~0.0002 W/m^2 heat signature of a Delivery Drone while it is efficiently processing data near the Landauer limit.

The Drone remains in encrypted radio contact with remote authorities, raising the risk of radio communications being detected by savvy adversaries. To avoid detection, the Drone might transmit only in short bursts or might use a frequency-hopping spread spectrum to minimize intercept risk. Thus the Drone communicates findings via a low-probability-of-intercept encrypted link to headquarters, or can store data on board for subsequent delivery or retrieval if transmissions during the mission might give it away.

Once all necessary data have been collected from a particular suspect facility and recorded in the computer memory of the Delivery Drone and the inspection devices, all devices can exit the facility and its vicinity, and report their results back to the APM Treaty Compliance Inspection Program authority for further action.

---

[179] Merkle RC, Freitas RA Jr., Hogg T, Moore TE, Moses MS, Ryley J. Molecular mechanical computing systems. IMM Report No 46, Apr 2016; http://www.imm.org/Reports/rep046.pdf.

[180] Bérut A, Arakelyan A, Petrosyan A, Ciliberto S, Dillenschneider R, Lutz E. Experimental verification of Landauer's principle linking information and thermodynamics. Nature. 2012 Mar 7;483(7388):187-189; https://www.nature.com/articles/nature10872.

[181] Landauer R. Irreversibility and heat generation in the computing process. IBM J Res Devel. 1961;5:183-191; http://fab.cba.mit.edu/classes/MAS.862/notes/computation/Landauer-1961.pdf. Bennett C, Landauer R. The fundamental physical limits of computation. Sci Am. 1985 Jul;253(1):48-57; http://web.eecs.umich.edu/~taustin/EECS598-HIC/public/Physical-Limits.pdf.

4. Representative Inspection Mission Scenario

The basic mission of the APM Treaty Compliance Inspection Program is to visit suspect facilities invisibly and unannounced and to inspect them for the presence or operation of proscribed nanotechnology equipment, including unauthorized atomically precise manufacturing facilities, their precursors, and their products. A representative mission scenario might unfold as follows:

1. **Create Mission Plan**. Select the next highest priority suspect facility inspection target on the list. Assemble publicly available information on the target facility, its personnel, its known nanotechnology activities, and the possible unlawful activities for which an inspection is required. Create a draft architectural model of the suspect facility using external photographs or maps of the site and any internal floor plans that might be publicly available. Create a comprehensive inspection plan to be conducted by inspection nanorobots. Manufacture and program all necessary inspection instrumentalities, including inspection nanorobots and drilling nanorobots, and load the Delivery Drone with this cargo.

2. **Deliver to Suspect Facility**. The Delivery Drone and its nanorobotic cargo are transported to within easy drone flight distance of the suspect facility. The Drone is unpacked and launched, flying to its destination in stealth mode, likely at low altitude and under cover of darkness. Upon arrival, the Delivery Drone parks in a predetermined inconspicuous location on the premises of the suspect facility from which it could operate unobserved for a period of up to several weeks if necessary.

3. **Deploy Mapping Robots**. The first wave of inspection nanorobots is deployed from the Delivery Drone. The robots proceed to predetermined entrances of the suspect facility and achieve entry by means previously described (Section 3.4.2). Once inside, inspection robots map all wall, floor, and ceiling surfaces in the facility to ~1 cm resolution (Section 3.3). Robots also map the location and gross surface structure of any unmoving objects in each room that could possibly represent a piece of proscribed equipment or which might need to be surveilled. Fixed landmarks are established for future nanorobot navigation, possibly including the placement of dedicated active landmarking robots. Nanorobots in each room monitor and record any regular spatial or temporal patterns of lighting (visual illumination) and human traffic to help plan stealth optimization during the next phase of operations. Innocuous electrical taps are installed in appropriate wall outlets to permit fast recharge by the next wave of inspection robots, and the locations of all such taps are recorded. Data-filled nanorobots return to the Delivery Drone, offload their information, receive new instructions, and then re-enter the facility to perform additional mapping and data collection tasks. For the largest facilities, multiple mapping cycles may be required over a period of up to 1 week to complete the facility map to the requisite level of accuracy and completeness.

4. **Compile Facility Map**. Computers on the Delivery Drone compile all data provided by the first wave of inspection nanorobots and create a systematic 3D architectural map of all floor, ceiling, and wall surfaces in the facility, identifying all features ≥1 cm in size. With assistance from remote resources with whom the Drone remains in encrypted radio contact (e.g., Treaty authority computers, databases, and personnel), a preliminary estimate is made of the identity and function of all unmoving objects found in all rooms, given the context of electrical and plumbing features near each object. Any possibly suspicious equipment is flagged and ranked in priority order for further detailed examination, based on probable relevance to the

search for unlawful APM activities and hardware. The Drone prepares a prioritized inspection plan and programs the nanorobots as appropriate for the second wave of inspection.

5. **Deploy Inspection Robots**. The second wave of inspection nanorobots is deployed from the Delivery Drone. These robots proceed to predetermined entrances of the suspect facility and achieve entry by means previously described (Section 3.4.2). Once inside, inspection robots in adequate numbers proceed to each target room and perform more detailed examination of all suspicious equipment in priority order, mapping the surfaces of all equipment in the facility to ~1 mm resolution (Section 3.4.1). Robots also perform a variety of inspection-justified surveillance activities such as monitoring and recording spoken conversations, recording data displayed on computer monitors, and the like (Section 3.4.1). The inspection fleet collects data of all kinds in the unconcealed observables category (Section 3.4), then exits the facility to download the information directly into the Delivery Drone computers. Nanorobots update their instructions and re-enter the facility to perform additional inspection and surveillance activities. For the largest facilities, multiple inspection cycles may be required over a period of 1 week or longer to acquire sufficient information to make a definitive determination of whether or not a Treaty violation has been observed. When this phase is complete, all inspection robots are withdrawn back to the Delivery Drone.

6. **Intrusive Inspection**. If it is determined, after local analysis and upon consultation with remote Treaty authority resources, that the inspection mission might have uncovered evidence that one or more rooms might harbor illegal equipment or activities but the existing data is insufficient to definitively rule out this possibility, then additional direct physical evidence must be collected.[182] The Drone prepares a more intrusive inspection process to collect new data in the concealed observables category (Section 3.5) and makes plans to obtain additional surveillance information from the communications and activities of suspect facility personnel. This process continues until enough data is available to form a definitive conclusion about the existence and extent of any Treaty violations. Once this is completed, all electrical taps are disassembled and removed, and all landmarking nanorobots are extracted. All remaining active inspection nanorobots are withdrawn back to the Delivery Drone and are securely stowed for travel.

7. **Drone Extraction**. The Delivery Drone and its nanorobotic cargo fly, in stealth mode and likely at low altitude and under cover of darkness, to a nearby airfield, mobile deployment system, or regional base operated by the APM Treaty Compliance Inspection authority, then is transported back to authority Headquarters for refurbishment and re-assignment to the next target suspect facility. If the Drone carries physical samples of possible APM material, these samples are delivered to the appropriate Treaty Compliance laboratory for further analysis. The results of such analysis might possibly mandate a re-inspection of the same suspect facility, or some alternative official response.

While it would clearly be possible to temporarily or permanently disable illegal equipment discovered in a suspect facility that is under investigation, the decision to undertake any such

---

[182] Treaty Compliance mission planners should consider using a Rolling Phase Mission Profile in which the waves overlap. As part of that approach, a good additional capability might be the capacity to call for a "reinforcement" Delivery Drone if or when needed.

aggressive action beyond the core inspection mission must reside outside of the purview of the APM Treaty Compliance Inspection Program authorities, and should not be initiated by them.

In summary, this exemplar scenario demonstrates that a covert inspection can successfully detect even well-hidden APM activities using the proposed nanorobotic tools and methods, all while minimizing exposure and without escalating to direct intervention. The information gained would then be handed off to the appropriate authorities for analysis and enforcement.